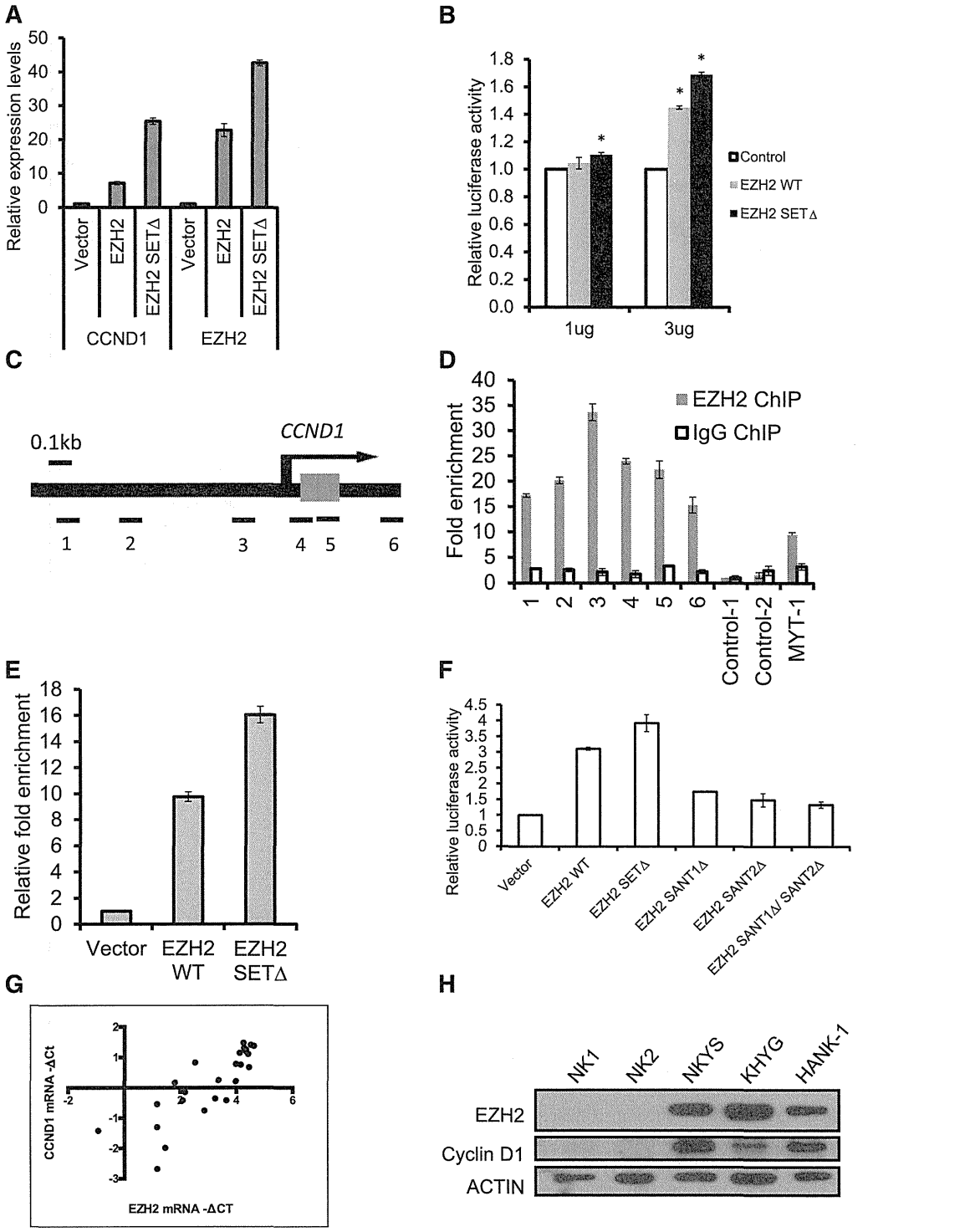

Figure 4. EZH2 positively regulates CCND1 transcription by binding to its promoter in NKTL cells. (A) Overexpression of EZH2 induces the expression of CCND1. Vectors expressing EZH2 (pcDNA-EZH2 or pcDNA-EZH2 SETΔ) were transiently transfected into NKYS cells. The RNA harvested from the cells at 24 hours after transfection was isolated, reverse-transcribed, subjected to qPCR by using primers specific for CCND1 mRNA, and normalized with GAPDH. (B) Luciferase promoter assay showing that EZH2 activates CCND1 transcription. NKYS cells were transfected with the luciferase reporter construct pGL4 containing the CCND1 promoter and various amounts of EZH2 WT/SETΔ plasmid or a control vector. Luciferase activities were measured after 24 hours. Luciferase readings were further normalized to the internal control pRL null. Results are presented as averages of triplicate experiments. Error bars represent standard deviation. * denotes $P < .01$ with respect to cells transfected with the same amount of control vector. (C) Genomic structure of human CCND1. The locations of the 6 pairs of primer sets used to detect the ChIP-enriched DNA fragments are indicated. (D) ChIP-qPCR for endogenous EZH2 binding to the CCND1 gene. ChIP assays were performed by using NKYS. Real-time PCR was performed with immunoprecipitated chromatin fragments obtained by using an anti-EZH2 antibody or an irrelevant antibody (IgG) as a control. A known EZH2 binding site in the promoter region of the MYT-1 gene was amplified as a positive control for the ChIP assays. (E) ChIP-qPCR for ectopically expressed EZH2 WT and EZH2 SETΔ binding to the CCND1 gene. ChIP assays were performed by using NKYS transfected by a pcDNA4.1/Myc-His vector or a plasmid expressing EZH2 WT and EZH2-SETΔ. Real-time PCR was performed with immunoprecipitated chromatin fragments obtained by using an anti-His antibody. Primer set 3, which amplifies a region representing EZH2 binding, was used to detect the ChIP-enriched DNA fragments. (F) Luciferase promoter assay showing the inability of EZH2 SANT domain deletion mutants to activate CCND1 transcription. NKYS were transfected with 3μg of EZH2 WT/SETΔ/SANTΔ plasmids or a control vector. Luciferase activities were measured after 24 hours. (G) Correlation between mRNA levels for EZH2 and CCND1 determined by qRT-PCR in NKTL clinical samples. Spearman correlation coefficient = 0.8608; $P < .0001$. (H) Western blot analysis of protein levels of CCND1 and EZH2 in NK cell lines and normal NK cells.

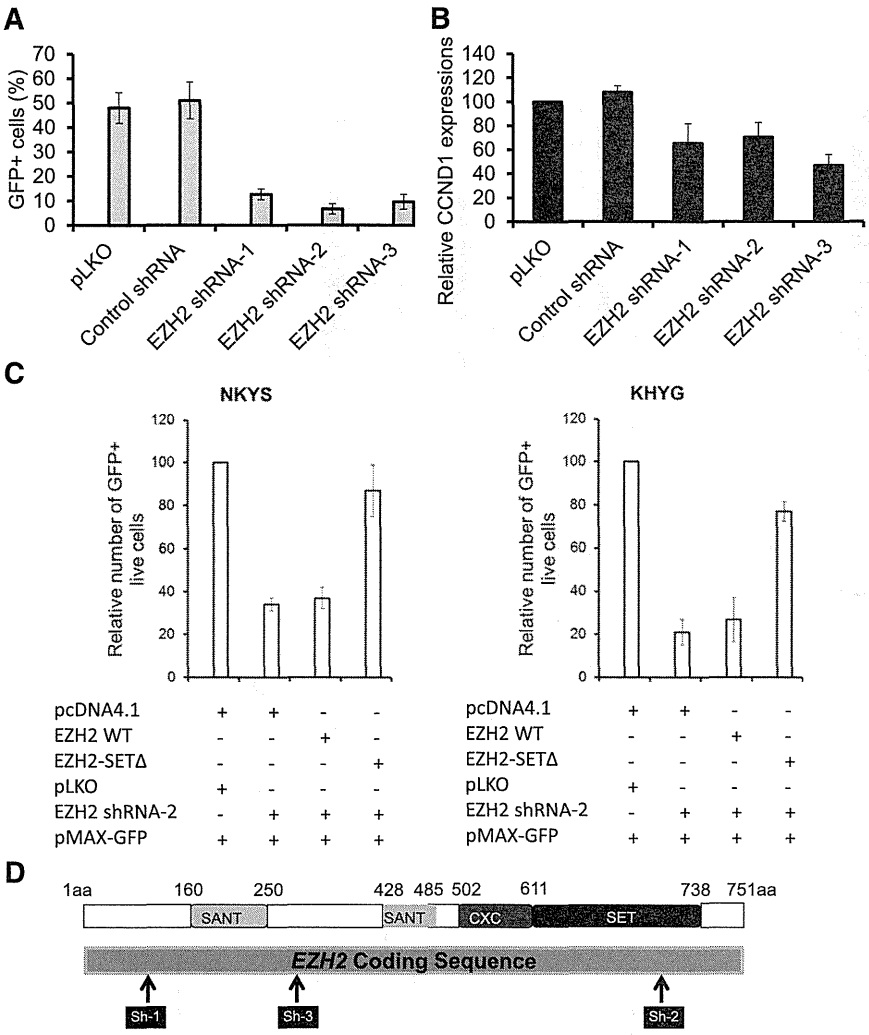

Figure 5. EZH2 depletion inhibits cell growth of NKTL tumor cells. (A) Effects of EZH2 knockdown on cell growth of NKYS cells. EZH2 shRNAs or control shRNA plasmids were cotransfected with a GFP-expressing plasmid pMAX-GFP in cells by electroporation. The percentage of GFP+ cells was determined by a Tali image-based cytometer at 18 hours after transfection. Cells transfected with EZH2 shRNA, but not those transfected with an empty vector or unrelated shRNA, exhibited a severe competitive growth disadvantage and cell death, as indicated by a significant depletion of GFP+ cells with time. (B) qRT-PCR analysis of CCND1 transcription in NKYS cells with EZH2 depleted by RNAi. (C) Rescue of EZH2 shRNA induced cell viability loss by forced expression of EZH2 SETΔ. Endogenous EZH2 was knocked down by an EZH2 shRNA-2, or was restored to physiological levels by ectopically expressing EZH2 shRNA2-resistant EZH2 SETΔ in NKYS and KHYG1 cells. Cells were cotransfected with EZH2 shRNA, together with either EZH2 WT or EZH2 SETΔ. Control transfections included a pLKO shRNA and pcDNA4.1, respectively. pMAX-GFP was cotransfected with other plasmids in each transfection to mark successfully transfected cells. The percentage of GFP+ live cells was determined by a Tali image-based cytometer at 18 hours after transfection. (D) Schematic description of EZH2 protein as well as the relative positions of regions targeted by EZH2 shRNAs. shRNAs expressed from a pLKO.1 vector targeting 3 regions of EZH2 are shown as black bars in relationship to the protein-coding regions.

compound capable of depleting PRC2 components called DZNep.[31] As reported previously,[31-34] DZNep effectively and dose-dependently reduced cellular levels of EZH2 in KHYG1 and NKYS, resulting in apoptosis as detected by PARP cleavage using western blot and Annexin V analysis by flow cytometry in a dose-dependent manner (Figure 6A,C). At the same time, CCND1 is down-regulated by DZNep at both the mRNA and protein levels (Figure 6A-B). In line with the diminished CCND1, NKYS treated with DZNep showed a substantial reduction in their proliferation rate, as illustrated by a 40% decrease in their BrdU incorporation (supplemental Figure 10). Thus, DZNep was able to phenocopy the effects of EZH2 knockdown on cell growth and CCND1 expression.

We next explored whether depletion of EZH2 is responsible for the cell growth inhibition and apoptosis observed by DZNep treatment in malignant NK cells. It is worth noting that DZNep depleted endogenous EZH2 protein but had no significant effect on exogenous EZH2 WT and EZH2 SETΔ (supplemental Figure 11). We observed a decrease in the DZNep-induced inhibition of cell growth in NKYS cells expressing both exogenous EZH2 WT and EZH2 SETΔ, compared with cells transfected with empty vector (Figure 6D). Although DZNep is not a specific inhibitor of EZH2 and may affect other molecules,[35] these findings indicate that DZNep-induced loss of cell viability in NKTL cells is, in large part, the result of a decrease in EZH2 levels.

Lastly, we evaluated the effects of DZNep on cell growth in other NK cell lines compared with normal NK cells. The MTS assay demonstrated that all of the additional 4 cell lines responded to DZNep treatment, whereas DZNep had minimal effects on normal NK cells (supplemental Figure 12A). Interestingly, the sensitivity of different cell lines to DZNep treatment seems to be related to EZH2 expression levels (supplemental Figure 12B).

Discussion

The data presented here show that EZH2 is aberrantly overexpressed in NKTL and that this is linked to Myc-mediated repression of miRNAs, such as miR26 and miR101 that normally target and inhibit EZH2 expression. This regulatory network demonstrated in NKTL further strengthens the recently proposed model that MYC may stimulate EZH2 overexpression by repression of its negative regulatory miRNAs.[9] Importantly, EZH2 overexpression is functionally important in NKTL, and the ability of EZH2 to promote proliferation in NKTL does not require its histone methyltransferase activity. Thus, for the first time our findings have uncovered a crucial and novel role for EZH2 in control of cell proliferation. Given our findings, it is likely that this unconventional role of EZH2

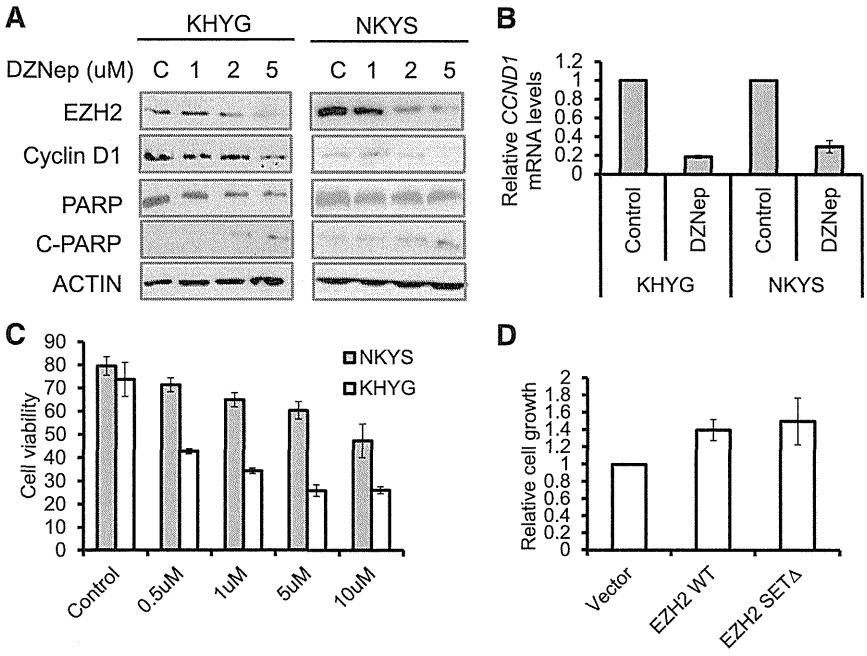

Figure 6. DZNep inhibits cell growth and induces apoptosis in NKTL tumor cells. (A) Western blot analysis of NK tumor cells exposed to increasing concentrations of DZNep showed a dose-dependent decrease in EZH2 protein, a decrease in CCND1 protein, and PARP cleavage in response to DZNep treatment. Cells were treated with indicated concentration of DZNep for 48 hours. Actin was used as a loading control. (B) Reduction of CCND1 mRNAs in DZNep-treated cells. The RNA harvested from the cells at 48 hours after treatment with DZNep at 5 μM, reverse-transcribed, subjected to qPCR by using primers specific for CCND1. (C) Quantification of cell viability in KHYG and NKYS cells treated with DZNep. Data are mean ±standard deviation of 3 independent experiments. (D) The rescued effects by EZH2 or EZH2Δ overexpression on DZNep-induced cell growth inhibition. Control plasmid or EZH2-expressing plasmids were cotransfected with pMAX-GFP to NKYS cells. Cells were then cultured in the absence or presence of DZNep at 10 μM for 48 hours. The percentage of GFP+ live cells was accessed by a Tali image-based cytometer.

seen in NTKL may represent a more general feature that may be also operational in other malignancies.

The best-understood mechanism by which EZH2 exerts its oncogenic function is to induce gene repression through its effect on chromatin via its histone methyltransferase activity that requires the SET domain of EZH2. However, there has been emerging evidence implying EZH2 functions that are not compatible with the transcription repression model. The oncogenic function of EZH2 has been attributed to the silencing of tumor suppressor genes such as *ARF*,[36] *p57KIP2*,[37] *FBXO32*,[38] *p27*,[33] and *BRCA1*.[39] Bracken and colleagues demonstrated that the downregulation of EZH2 expression by RNAi did not increase the expression of these negative regulators of the cell cycle.[27] On the other hand, there was a significant decrease in the positive regulators of cell proliferation such as G1/*S*-expressed cyclins in EZH2 knockdown cells.[27] These observations suggest that EZH2 is required for activation or maintenance of the activated state of certain genes in proliferating cells. The first evidence indicating a role of EZH2 in transcriptional activation was provided by Shi and colleagues[40] in which EZH2 interacts directly with estrogen receptor and β-catenin, functionally enhancing gene transactivation in the estrogen and Wnt pathways. In a more recent study, we demonstrated that EZH2 in aggressive breast cancer cells can positively modulate the NF-κB target gene by forming a ternary complex with RelA and RelB.[30] Notably, both studies demonstrated that this transcriptional activation activity is independent of the EZH2 SET domain and H3K27me3, although neither study has provided a phenotypic demonstration of such a histone methyltransferase–independent function of EZH2. Our results here clearly demonstrate that EZH2 enhances proliferation of malignant NK cells without requiring its enzyme activity, which highlights a mechanism not well recognized for EZH2 function.

Recent reports increasingly suggest an important role of EZH2 in a wide range of hematologic malignancies, yet its exact tumorigenic role and mechanism and the pathways it deregulates seem to vary in different malignancies. For example, we recently showed that EZH2 enzymatic function in acute myeloid leukemia is important and may be involved in deregulating metabolic pathway genes.[34] On the other hand, in the current study in NKTL, the nonenzymatic mechanism seems to be important in driving cell cycle progression by activating CCND1 expression. The understanding of how EZH2 works as an oncogene in different cancers has important therapeutic implications. EZH2 is currently thought to be important in oncogenesis through its enzymatic activity; hence, inhibitors in development are mostly targeting EZH2 enzymatic activity. Our study demonstrates that the oncogenic function of EZH2 may not always be dependent on its enzymatic activities. Therefore, small-molecule drugs that block EZH2 enzymatic activity will not work in these situations. This implies a need to review current therapeutic strategies. In view of the dual function of EZH2 in transcription activation and epigenetic repression, ideally there is a need to identify tumors where EZH2 is predominantly acting through its enzymatic function as a histone methyltransferase, inhibiting the protective role of tumor suppressor genes, as well as tumors where EZH2 is predominantly acting through activation of genes involved in other oncogenic pathways. This will ensure that the appropriate therapeutic strategy can be applied. Conversely, a compound that downregulates EZH2 protein may be effective in both scenarios. Therefore, therapeutic compounds that lead to EZH2 protein degradation rather than specific enzymatic inhibitors may be advantageous.

The proproliferative properties of EZH2 in NKTL support the rationale for using EZH2 inhibitors in the treatment of NKTL. Because targeting of EZH2 is an active area of drug development at present, there is great potential for the development of better treatment modalities. This is especially important for aggressive cancers, such as NKTL, for which no effective curative treatment is currently available.

Acknowledgments

The authors thank Prof. Daniel G. Tenen and Prof. H. Phillip Koeffler for their helpful suggestions.

W.-J.C. was supported by the National Medical Research Council Clinician Scientist Investigator Award. This work is supported in

part by the Singapore National Research Foundation and the Ministry of Education under the Research Center of Excellence Program to W.-J.C. S.-B.N. was supported by the National University Health System Clinician Scientist Program Award.

Authorship

Contribution: J.Y. and W.-J.C. conceived and designed the study, analyzed and interpreted the data, and wrote the paper; Q.Y. provided vital reagents and interpreted findings; S.-B.N. provided clinical samples, performed IHC scoring, interpreted the data, and wrote the paper; S.W. performed IHC scoring; J.Y., J.L.-S.T., B.L., T.L.K., J.T., V.S., S.-C.L., C.B., and S.-N.C. performed experiments; G.H. performed bioinformatics analysis; and N.S. contributed the cell lines.

Conflict-of-interest disclosure: The authors declare no competing financial interests.

Correspondence: Wee-Joo Chng, Department of Hematology-Oncology, National University Cancer Institute of Singapore, National University Health System, 1E, Kent Ridge Rd, Singapore 119228; e-mail: mdccwj@nus.edu.sg.

References

1. Lee J, Suh C, Park YH, et al. Extranodal natural killer T-cell lymphoma, nasal-type: a prognostic model from a retrospective multicenter study. *J Clin Oncol.* 2006;24(4):612-618.
2. Jaccard A, Hermine O. Extranodal natural killer/T-cell lymphoma: advances in the management. *Curr Opin Oncol.* 2011;23(5):429-435.
3. Gill H, Liang RH, Tse E. Extranodal natural-killer/t-cell lymphoma, nasal type. *Adv Hematol.* 2010;2010:627401.
4. Ng SB, Selvarajan V, Huang G, et al. Activated oncogenic pathways and therapeutic targets in extranodal nasal-type NK/T cell lymphoma revealed by gene expression profiling. *J Pathol.* 2011;223(4):496-510.
5. Bracken AP, Dietrich N, Pasini D, Hansen KH, Helin K. Genome-wide mapping of Polycomb target genes unravels their roles in cell fate transitions. *Genes Dev.* 2006;20(9):1123-1136.
6. Chang CJ, Hung MC. The role of EZH2 in tumour progression. *Br J Cancer.* 2012;106(2):243-247.
7. Richter GH, Plehm S, Fasan A, et al. EZH2 is a mediator of EWS/FLI1 driven tumor growth and metastasis blocking endothelial and neuro-ectodermal differentiation. *Proc Natl Acad Sci USA.* 2009;106(13):5324-5329.
8. Chang CJ, Yang JY, Xia W, et al. EZH2 promotes expansion of breast tumor initiating cells through activation of RAF1-β-catenin signaling. *Cancer Cell.* 2011;19(1):86-100.
9. Sander S, Bullinger L, Klapproth K, et al. MYC stimulates EZH2 expression by repression of its negative regulator miR-26a. *Blood.* 2008;112(10):4202-4212.
10. Varambally S, Cao Q, Mani RS, et al. Genomic loss of microRNA-101 leads to overexpression of histone methyltransferase EZH2 in cancer. *Science.* 2008;322(5908):1695-1699.
11. Cha TL, Zhou BP, Xia W, et al. Akt-mediated phosphorylation of EZH2 suppresses methylation of lysine 27 in histone H3. *Science.* 2005;310(5746):306-310.
12. Wei Y, Chen YH, Li LY, et al. CDK1-dependent phosphorylation of EZH2 suppresses methylation of H3K27 and promotes osteogenic differentiation of human mesenchymal stem cells. *Nat Cell Biol.* 2011;13(1):87-94.
13. Morin RD, Johnson NA, Severson TM, et al. Somatic mutations altering EZH2 (Tyr641) in follicular and diffuse large B-cell lymphomas of germinal-center origin. *Nat Genet.* 2010;42(2):181-185.
14. Yap DB, Chu J, Berg T, et al. Somatic mutations at EZH2 Y641 act dominantly through a mechanism of selectively altered PRC2 catalytic activity, to increase H3K27 trimethylation. *Blood.* 2011;117(8):2451-2459.
15. McCabe MT, Graves AP, Ganji G, et al. Mutation of A677 in histone methyltransferase EZH2 in human B-cell lymphoma promotes hypertrimethylation of histone H3 on lysine 27 (H3K27). *Proc Natl Acad Sci USA.* 2012;109(8):2989-2994.
16. Nikoloski G, Langemeijer SM, Kuiper RP, et al. Somatic mutations of the histone methyltransferase gene EZH2 in myelodysplastic syndromes. *Nat Genet.* 2010;42(8):665-667.
17. Ernst T, Chase AJ, Score J, et al. Inactivating mutations of the histone methyltransferase gene EZH2 in myeloid disorders. *Nat Genet.* 2010;42(8):722-726.
18. Ntziachristos P, Tsirigos A, Van Vlierberghe P, et al. Genetic inactivation of the polycomb repressive complex 2 in T cell acute lymphoblastic leukemia. *Nat Med.* 2012;18(2):298-301.
19. Ng SB, Yan J, Huang G, et al. Dysregulated microRNAs affect pathways and targets of biologic relevance in nasal-type natural killer/T-cell lymphoma. *Blood.* 2011;118(18):4919-4929.
20. Feng M, Li Z, Aau M, Wong CH, Yang X, Yu Q. Myc/miR-378/TOB2/cyclin D1 functional module regulates oncogenic transformation. *Oncogene.* 2011;30(19):2242-2251.
21. Chen X, Xu H, Yuan P, et al. Integration of external signaling pathways with the core transcriptional network in embryonic stem cells. *Cell.* 2008;133(6):1106-1117.
22. Iqbal J, Kucuk C, Deleeuw RJ, et al. Genomic analyses reveal global functional alterations that promote tumor growth and novel tumor suppressor genes in natural killer-cell malignancies. *Leukemia.* 2009;23(6):1139-1151.
23. Guo H, Ingolia NT, Weissman JS, Bartel DP. Mammalian microRNAs predominantly act to decrease target mRNA levels. *Nature.* 2010;466(7308):835-840.
24. Chang TC, Yu D, Lee YS, et al. Widespread microRNA repression by Myc contributes to tumorigenesis. *Nat Genet.* 2008;40(1):43-50.
25. Holm K, Grabau D, Lövgren K, et al. Global H3K27 trimethylation and EZH2 abundance in breast tumor subtypes. *Mol Oncol.* 2012;6(5):494-506.
26. Wei Y, Xia W, Zhang Z, et al. Loss of trimethylation at lysine 27 of histone H3 is a predictor of poor outcome in breast, ovarian, and pancreatic cancers. *Mol Carcinog.* 2008;47(9):701-706.
27. Bracken AP, Pasini D, Capra M, Prosperini E, Colli E, Helin K. EZH2 is downstream of the pRB-E2F pathway, essential for proliferation and amplified in cancer. *EMBO J.* 2003;22(20):5323-5335.
28. Huang Y, de Reyniès A, de Leval L, et al. Gene expression profiling identifies emerging oncogenic pathways operating in extranodal NK/T-cell lymphoma, nasal type. *Blood.* 2010;115(6):1226-1237.
29. Cao W, Liu Y, Zhang H, et al. Expression of LMP-1 and Cyclin D1 protein is correlated with an unfavorable prognosis in nasal type NK/T cell lymphoma. *Mol Med Rep.* 2008;1(3):363-368.
30. Lee ST, Li Z, Wu Z, et al. Context-specific regulation of NF-κB target gene expression by EZH2 in breast cancers. *Mol Cell.* 2011;43(5):798-810.
31. Tan J, Yang X, Zhuang L, et al. Pharmacologic disruption of Polycomb-repressive complex 2-mediated gene repression selectively induces apoptosis in cancer cells. *Genes Dev.* 2007;21(9):1050-1063.
32. Xie Z, Bi C, Cheong LL, et al. Determinants of sensitivity to DZNep induced apoptosis in multiple myeloma cells. *PLoS ONE.* 2011;6(6):e21583.
33. Fiskus W, Wang Y, Sreekumar A, et al. Combined epigenetic therapy with the histone methyltransferase EZH2 inhibitor 3-deazaneplanocin A and the histone deacetylase inhibitor panobinostat against human AML cells. *Blood.* 2009;114(13):2733-2743.
34. Zhou J, Bi C, Cheong LL, et al. The histone methyltransferase inhibitor, DZNep, up-regulates TXNIP, increases ROS production, and targets leukemia cells in AML. *Blood.* 2011;118(10):2830-2839.
35. Miranda TB, Cortez CC, Yoo CB, et al. DZNep is a global histone methylation inhibitor that reactivates developmental genes not silenced by DNA methylation. *Mol Cancer Ther.* 2009;8(6):1579-1588.
36. Bracken AP, Kleine-Kohlbrecher D, Dietrich N, et al. The Polycomb group proteins bind throughout the INK4A-ARF locus and are disassociated in senescent cells. *Genes Dev.* 2007;21(5):525-530.
37. Yang X, Karuturi RK, Sun F, et al. CDKN1C (p57) is a direct target of EZH2 and suppressed by multiple epigenetic mechanisms in breast cancer cells. *PLoS ONE.* 2009;4(4):e5011.
38. Wu Z, Lee ST, Qiao Y, et al. Polycomb protein EZH2 regulates cancer cell fate decision in response to DNA damage. *Cell Death Differ.* 2011;18(11):1771-1779.
39. Gonzalez ME, Li X, Toy K, et al. Downregulation of EZH2 decreases growth of estrogen receptor-negative invasive breast carcinoma and requires BRCA1. *Oncogene.* 2009;28(6):843-853.
40. Shi B, Liang J, Yang X, et al. Integration of estrogen and Wnt signaling circuits by the polycomb group protein EZH2 in breast cancer cells. *Mol Cell Biol.* 2007;27(14):5105-5119.

Clinical Investigations

Respiration

Respiration
DOI: 10.1159/000355200

Received: May 18, 2013
Accepted after revision: August 19, 2013
Published online: December 7, 2013

Detection of Herpes Viruses by Multiplex and Real-Time Polymerase Chain Reaction in Bronchoalveolar Lavage Fluid of Patients with Acute Lung Injury or Acute Respiratory Distress Syndrome

Ryo Tachikawa[a] Keisuke Tomii[a] Ryutaro Seo[b] Kazuma Nagata[a] Kyoko Otsuka[a] Atsushi Nakagawa[a] Kojiro Otsuka[a] Hisako Hashimoto[c] Ken Watanabe[d] Norio Shimizu[d]

Departments of [a]Respiratory Medicine and [b]Critical Care, Kobe City Medical Center General Hospital, and [c]Department of Cell Therapy, Institute of Biomedical Research and Innovation, Kobe, and [d]Virology, Medical Research Institute, Tokyo Medical and Dental University, Tokyo, Japan

Key Words

Acute lung injury · Acute respiratory distress syndrome · Human herpes virus · Multiplex polymerase chain reaction · Real-time polymerase chain reaction

Abstract

Background: Human herpes viruses (HHVs) are important pathogens in acute lung injury (ALI) and acute respiratory distress syndrome (ARDS). Rapid and efficient diagnostic tools are needed to detect HHVs in the lung in ALI/ARDS patients. ***Objectives:*** This study aimed to evaluate the usefulness of multiplex and real-time polymerase chain reaction (PCR) analysis of bronchoalveolar lavage fluid (BALF) for detecting HHV reactivation in ALI/ARDS patients. ***Methods:*** Between August 2008 and July 2012, eighty-seven BALF samples were obtained from ALI/ARDS patients with unknown etiology and analyzed for HHVs. The types of HHVs in the BALF samples were determined using qualitative multiplex PCR followed by quantitative real-time PCR. ***Results:*** Multiplex PCR identified herpes simplex virus type 1 (HSV-1) (n = 11), Epstein-Barr virus (EBV) (n = 16), cytomegalovirus (CMV) (n = 21), HHV type 6 (HHV-6) (n = 2), and HHV-7 (n = 1) genomic DNA in 35 (40%) of the BALF samples, including 14 (16%) samples containing 2 or 3 HHV types. CMV and EBV reactivation was rare in immunocompetent patients, whereas reactivation of HSV-1 was predominantly observed in intubated patients regardless of their immune status. Overall, HHVs were almost exclusively found in patients with immunosuppression or endotracheal intubation. Real-time PCR detected 0.95–1.59 × 10^6 copies of viral DNA/μg human genome DNA, and HSV-1 (n = 4), CMV (n = 9), and HHV-6 (n = 1) were identified as potentially pathogenic agents. ***Conclusions:*** The implementation of multiplex and real-time PCR of BALF was feasible in ALI/ARDS patients, which allowed efficient detection and quantification of HHV DNA.

Introduction

Acute lung injury (ALI) and acute respiratory distress syndrome (ARDS) remain critical illnesses with substantial morbidity and mortality [1]. Despite advances in understanding the pathophysiology of ALI/ARDS, the

KARGER

E-Mail karger@karger.com
www.karger.com/res

0025–7931/13/0000–0000$38.00/0

Ryo Tachikawa, MD
Department of Respiratory Medicine
Kobe City Medical Center General Hospital
2-1-1, Minatojima-minamimachi, Chuo-ku, Kobe 650-0047 (Japan)
E-Mail ryotkw@gmail.com

mainstay of treatment for these diseases primarily involves supportive care and management of the underlying clinical disorder. Therefore, the pathogenic factors underlying these medical conditions need to be identified to indicate potential therapeutic interventions.

Human herpes viruses (HHVs) have been recognized as clinically important pathogens of pulmonary infections that can result in ALI/ARDS in immunocompromised patients [2–4], and they have also been recognized as potential pathogens in nonimmunocompromised critically ill patients [5–9]. However, there have been few comprehensive studies to date on the prevalence and pathogenic role of HHVs in ALI/ARDS patients, partly due to the limited diagnostic tools available for identifying different HHVs in a clinical sample.

In recent years, development of the multiplex polymerase chain reaction (PCR) assay has enabled simultaneous detection of a wide range of viruses [10]. Although a positive PCR for HHVs does not distinguish asymptomatic shedding from an active infection, quantification of the viral load in bronchoalveolar lavage fluid (BALF) could potentially differentiate between these two conditions [6, 11–13]. Therefore, rapid screening of BALF by qualitative multiplex PCR to identify virus-positive samples followed by quantitative PCR of the positive samples may be a useful diagnostic approach for evaluating lung diseases possibly caused by HHVs.

The aim of the present study was to evaluate the usefulness of multiplex and real-time PCR analysis of BALF for detecting HHV reactivation in ALI/ARDS patients.

Methods

Patients and Clinical Samples

Between August 2008 and July 2012, a total of 134 diagnostic bronchoalveolar lavage (BAL) procedures were performed in new-onset ALI/ARDS patients when the etiology of ALI/ARDS was unknown and was unlikely to be caused by bacterial pneumonia based on the clinical presentation, radiological findings, or the response to antibiotics. Of these, 87 BALF samples were analyzed for HHVs using multiplex PCR as part of the diagnostic examination, and the data were retrospectively examined in this study. BAL sampling was carried out via standard techniques, usually instilling five 30-ml aliquots of normal saline, and the specimens were stored at −80°C until the PCR was performed. The BALF was routinely tested for common pathogens (bacteria, fungi, and *Mycobacterium*) and for viral inclusion bodies by cytology. Additional microbiological studies, including quantitative PCR for *Pneumocyctis jirovecii* in BALF and cytomegalovirus (CMV) pp65 antigen levels in blood were performed as appropriate. Clinical and laboratory data were also collected from medical records. This study was approved by our institutional review board.

Classification of Viral Pneumonia Cases and Clinical Definitions

Classification of viral pneumonia cases was based on viral detection in BALF and on the following criteria: (1) proven viral pneumonia: specific cytopathic effects (inclusion bodies) in cells from BALF or transbronchial biopsy, (2) probable viral pneumonia: otherwise unexplained ALI/ARDS with a clinical response to specific antiviral agents, and (3) possible viral pneumonia: viral load $>10^4$ copies/μg DNA in BALF, otherwise unexplained ALI/ARDS, and antiviral agents ineffective or not administered. In possible viral pneumonia cases, there may be a clinical response to specific antiviral agents administered concurrently with efficacious treatments for known causes of ALI/ARDS. ALI/ARDS was defined according to previously reported criteria [14]. An immunocompromised patient was defined as one receiving immunosuppressants or corticosteroid therapy for more than 1 month or having AIDS.

PCR Analysis

HHV genomic DNA was measured by two independent PCR assays: qualitative multiplex PCR followed by quantitative real-time PCR of the HHV-positive samples detected by multiplex PCR.

The multiplex PCR was designed to identify the genomic DNA of 8 HHVs: herpes simplex virus type 1 (HSV-1), HSV-2, varicella zoster virus (VZV), Epstein-Barr virus (EBV), CMV, HHV type 6 (HHV-6), HHV-7, and HHV-8. DNA extraction was performed on 200- to 400-μl BALF samples using E21 virus minikits (Qiagen Inc., Valencia, Calif., USA). The multiplex PCR amplifications were set up in 2 capillaries (capillary 1: HSV-1, HSV-2, VZV, CMV, and HHV-6; capillary 2: EBV, HHV-7, and HHV-8), each containing 5 μl DNA extract, specific primers, hybridization probe mix, and Accuprime Taq (Invitrogen, Carlsbad, Calif., USA). The primers and probes for HHVs have been described previously [15] and are shown in table 1. The reactions were performed using the LightCycler PCR System (Roche, Switzerland) with the following conditions: an initial denaturation step at 95°C for 2 min, followed by 40 cycles at 95°C for 2 s, 58°C for 15 s, and 72°C for 15 s, with a final extension at 40°C for 30 s. Hybridization probes were then mixed with the PCR products and melting curves were analyzed using the LightCycler System. The sensitivity of the multiplex PCR analysis was 50 copies/tube.

Subsequently, for HHV-positive samples, real-time PCR was performed to measure the viral load using Amplitaq Gold and the Real-Time PCR 7300 System (ABI, Foster City, Calif., USA). The sequences of the primers and probes for the HHVs and the PCR conditions used in this study have been previously reported [16]. The BALF samples were also analyzed by PCR for the housekeeping gene glyceraldehyde-3-phosphate dehydrogenase (GAPDH) as an internal control, and the number of viral DNA copies was calculated as copies per microgram of human genome DNA. The viral DNA in the blood samples of selected patients was measured using the same multiplex PCR conditions, and the results were calculated as copies per milliliter of whole blood.

Statistics

Continuous variables are expressed as means ± SD unless stated otherwise. Categorical variables were compared using the χ^2 test or Fisher's exact test as appropriate. The CMV viral load in BALF was assessed as a diagnostic test for CMV pneumonia us-

Table 1. Sequences of primers and probes used in the multiplex PCR

Virus	Target gene	Primer sequence	Probe sequence
HSV-1, HSV-2[a]	polymerase	F: GCTCGAGTGCGAAAAAACGTTC R: TGCGGTTGATAAACGCGCAGT	3′FITC: GCGCACCAGATCCACGCCCTTGATGAGC LcRed604-5′: CTTGCCCCCGCAGATGACGCC
VZV	gene 29	F: TGTCCTAGAGGAGGTTTTATCTG R: CATCGTCTGTAAAGACTTAACCAG	3′FITC: GGGAAATCGAGAAACCACCCTATCCGAC LcRed640-5′: AAGTTCGCGGTATAATTGTCAGT
EBV	BamH1	F: CGCATAATGGCGGACCTAG R: CAAACAAGCCCACTCCCC	3′FITC: AAAGATAGCAGCAGCGCAGC LcRed640-5′: AACCATAGACCCGCTTCCTG
CMV	CMV glycoprotein	F: TACCCCTATCGCGTGTGTTC R: ATAGGAGGCGCCACGTATTC	3′FITC: TCGTCGTAGCTACGCTTACAT LcRed705-5′: ACACCACTTATCTGCTGGGCAGC
HHV-6	101k gene region	F: ACCCGAGAGATGATTTTGCG R: GCAGAAGACAGCAGCGAGTA	3′FITC: TAAGTAACCGTTTTCGTCCCA LcRed705-5′: GGGTCATTTATGTTATAGA
HHV-7	U57	F: GAAAAATCCGCCATAATAGC R: ATGGAACACCTATTAACGGC	3′FITC: GCCATAAGAAACAGGTACAGACATTGTCA LcRed705-5′: TTGTGAAATGTGTTGCG
HHV-8	EB BDLF1 ORF26	F: AGCCGAAAGGATTCCACCAT R: TCCGTGTTGTCTACGTCCAG	3′FITC: CCGGATGATGTAAATATGGCGGAAC LcRed705-5′: TGATCTATATACCACCAATGTGTCATTTATG

F = Forward primer; R = reverse primer.

[a] The primer sequences were the same for both HSV-1 and HSV-2, while the probe sequences were a complete match with the HSV-2 genome sequence but had a two-base mismatch with the HSV-1 genome sequence. Therefore, there was a difference in melting temperature between HSV-1 and HSV-2, enabling discrimination of these two viruses.

ing a receiver operating characteristic plot. $p < 0.05$ was considered statistically significant. All statistical analyses were performed using JMP 7.0.2 software (SAS Institute Inc., Cary, N.C., USA).

Results

Study Population

The clinical characteristics of the patients in this study are summarized in table 2. The underlying conditions were diverse and 49 (56%) patients were immunocompromised. ALI/ARDS developed in a nosocomial setting in 31 (35%) patients. Predominant ground-glass opacity mixed with focal air space consolidation was the most frequent radiological finding.

Viral Detection in BALF

The HHV virology results are summarized in table 3. Multiplex and real-time PCR detected HSV-1 in 11 (13%) BALF samples (2.92×10^2–6.22×10^5 copies/μg DNA), EBV in 16 (18%) samples (9.50×10^{-1}–6.62×10^4 copies/μg DNA), CMV in 21 (24%) samples (2.55–1.59×10^6 copies/μg DNA), HHV-6 in 2 (2%) samples (6.90×10^4–6.90×10^6 copies/μg DNA), and HHV-7 in 1 (1%) sample (3.12×10^3 copies/μg DNA). HSV-2, VZV, and HHV-8 were not detected. Overall, 35 (40%) patients were positive for at least one type of HHV, and multiple HHV types were detected in 14 (16%) patients.

The prevalence of HSV-1 was higher in intubated patients than in nonintubated patients (41 vs. 3%, $p < 0.0001$), but it was not significantly different between immunocompromised and immunocompetent patients (12 vs. 13%, $p = 0.90$) (fig. 1). In contrast, in CMV- and EBV-positive patients, the prevalence of CMV (fig. 2) and EBV (fig. 3) was not significantly different between intubated patients (31 and 18%, respectively) and nonintubated patients (22 and 18%, respectively) ($p = 0.33$ and $p = 1.00$, respectively), but it was significantly higher in immunocompromised patients (39 and 29%, respectively) than in immunocompetent patients (5 and 5%, respectively) ($p = 0.0003$ and $p = 0.006$, respectively). HHV-6- and HHV-7-positive BALF was obtained from immunocompromised patients. Overall, the prevalence of HHVs was higher in immunocompromised and/or intubated patients (55%; 32/58) than in immunocompetent patients without endotracheal intubation (10%; 3/29) ($p < 0.0001$).

Table 2. Baseline characteristics of the 87 patients in this study

Age, years	64.3±14.3
Male gender, n (%)	59 (68)
Underlying disease, n (%)	
Connective tissue disease	19 (22)
Posttransplant	9 (10)
Hematologic malignancy	8 (9)
Solid cancer	8 (9)
Postoperative	3 (3)
Hemodialysis	3 (3)
AIDS	2 (2)
Underlying pulmonary disease, n (%)	
IIP	21 (24)
CTD-IP	6 (7)
Immunocompromised, n (%)	49 (56)
Nosocomial onset, n (%)	31 (35)
Mechanical ventilation, n (%)	
At the time of BAL	27 (31)
Over the course of hospitalization	61 (70)
PaO_2/FIO_2, mm Hg	163±68.7
ALI, n (%)	28 (32)
ARDS, n (%)	59 (68)
Duration of symptoms, days	9.7±9.6
LDH, IU/l	543±363
CRP, mg/dl	10.3±3.3
CT findings (%)	
GGO only	12 (14)
GGO predominant	62 (71)
Consolidation predominant	13 (15)
BALF samples[a]	
Median total cell count (range), n × 10^5/mm^3	2.35 (0.1–88.8)
Median neutrophils (range), %	28 (0–93)
Median lymphocytes (range), %	15 (1–82)
Median eosinophils (range), %	1 (0–46)
Median macrophages (range), %	32 (0–84)

IIP = Idiopathic interstitial pneumonia; CRP = C-reactive protein; LDH = lactate dehydrogenase; CTD-IP = connective tissue disease-associated interstitial pneumonia; GGO = ground-glass opacity.

[a] Fiberoptic bronchoscopy was performed with supplemental oxygen (n = 23), under noninvasive ventilation (n = 42), or under endotracheal intubation (n = 22).

Diagnosis

Fourteen patients in this study were diagnosed with viral pneumonia: 9 with CMV pneumonia (5 proven, 3 probable, 1 possible viral pneumonia), 4 with HSV-1 pneumonia (all possible viral pneumonia), and 1 with HHV-6 pneumonia (probable viral pneumonia) (table 4). Diagnoses of the other patients included acute exacerbation of interstitial pneumonia (n = 18), pneumocystis pneumonia (n = 13), other pulmonary infections (n = 7), diffuse alveolar hemorrhage (n = 7), septic ARDS (n = 3), drug-induced pneumonia (n = 3), other causes of ALI/ARDS (n = 11), and unidentified etiology (n = 12). HHVs were not detected in the BALF of patients with acute exacerbation of interstitial pneumonia, except in one BALF that had a low EBV viral load (278 copies/μg DNA). For a diagnosis of proven or probable CMV pneumonia, a cutoff value for the viral load in BALF of 1.39×10^4 copies/μg DNA had 87.5% sensitivity and 84.6% specificity.

Treatment and Outcome

Antiviral agents were administered to 13 patients with a diagnosis of viral pneumonia. Although respiratory improvement was seen, at least temporally, in 9 of the patients diagnosed with CMV or HHV-6 pneumonia, 10 (77%) patients eventually died due to a newly acquired infection, sustained respiratory failure, or multiorgan dysfunction (table 4). The overall in-hospital mortality in this cohort was 51%.

Discussion

This study showed that multiplex PCR and real-time PCR analysis of HHVs in BALF provided informative data regarding the epidemiologic characteristics of HHVs in ALI/ARDS patients with unknown etiology. To our knowledge, this is the first study to conduct comprehensive multiplex and real-time PCR analyses of HHVs in BALF of ALI/ARDS patients.

Viruses in the Herpesviridae family are the most common viral pathogens causing pulmonary infection in immunocompromised patients. Although CMV is best known for its propensity to cause pneumonia [2], other herpes viruses (e.g. HSV-1 [3, 17], VZV [18], EBV [19], and HHV-6 [20, 21]) have also been implicated as etiologic agents. Moreover, recent studies have documented frequent pulmonary reactivation and/or infection of HSV-1 [6, 7] and CMV [8, 9] in critically ill patients with no known immunocompromise. Therefore, ALI/ARDS patients with unknown etiology should be examined for possible viral pneumonia caused by HHVs, which often presents with bilateral ground-glass opacification and/or consolidation [17, 21, 22]. In this setting, the diagnosis must be broadened to a wide range of HHVs that can be efficiently examined by multiplex PCR instead of conventional microbiological tests for specific pathogens. In fact, this study found reactivation of 5 types of herpes viruses in 40% of ALI/ARDS patients, including 16% of patients with multiple types of HHVs in their BALF.

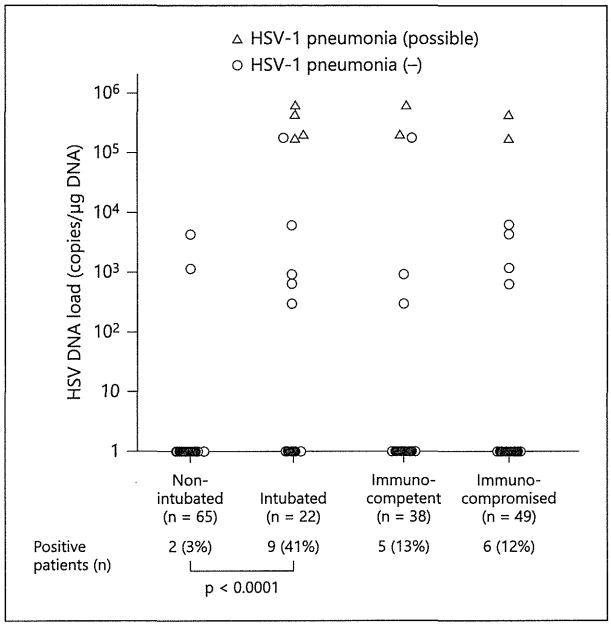

Fig. 1. HSV-1 prevalence and semi-log plot of the HSV-1 DNA load in BALF as a function of patient intubation or immune status. Negative PCR results were set to 1 ($\log_{10}$ 1 = 0).

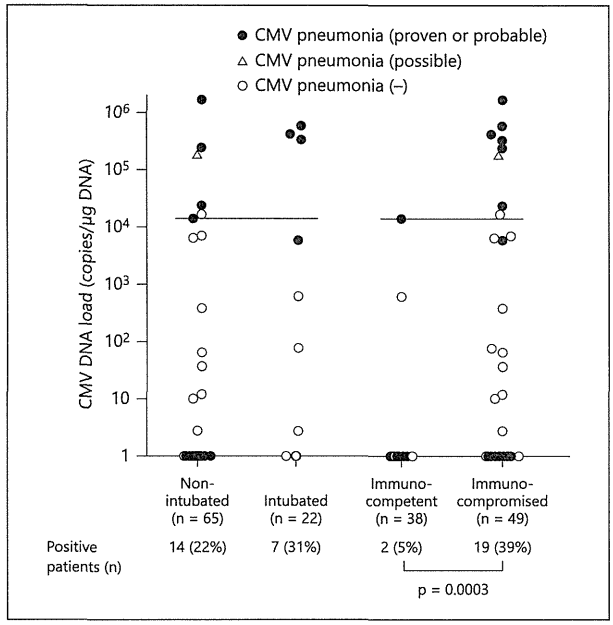

Fig. 2. CMV prevalence and semi-log plot of the CMV DNA load in BALF as a function of patient intubation or immune status. Negative PCR results were set to 1 ($\log_{10}$ 1 = 0). The bar represents the cutoff value indicating CMV pneumonia (1.39×10^4 copies/μg DNA).

Table 3. HHV prevalence and viral load in BALF samples from the 87 patients in this study

	HSV-1	HSV-2	VZV	EBV	CMV	HHV-6	HHV-7	HHV-8
Positive BALF[a], n (%)	11 (13)	0	0	16 (18)	21 (24)	2 (2)	1 (1)	0
Viral load, copies/μg DNA	2.92×10^2–6.22×10^5	–	–	9.50×10^{-1}–6.62×10^4	2.55–1.59×10^6	6.90×10^4–6.90×10^6	3.12×10^3	–
BALF samples with a viral load, n								
≥0	0	–	–	2	3	0	0	–
≥10	0	–	–	2	4	0	0	–
$\geq10^2$	3	–	–	5	2	0	0	–
$\geq10^3$	3	–	–	3	3	0	1	–
$\geq10^4$	0	–	–	4	3	1	0	–
$\geq10^5$	5	–	–	0	5	0	0	–
$\geq10^6$	0	–	–	0	1	1	0	–

[a] Two types of HHVs were detected in 12 samples (EBV and CMV in 6, HSV-1 and EBV in 3, HSV-1 and CMV in 2, and CMV and HHV-6 in 1). Three types of HHVs were detected in 2 samples (EBV, CMV, and HHV-7 in 1 and HSV-1, EBV, and CMV in 1).

Considering the diversity of HHVs detected in this study, multiplex PCR has the additional advantage of being able to identify unexpected agents that might otherwise be overlooked, thereby enabling early therapeutic intervention.

This study provided insights into the epidemiologic features of herpes viruses in ALI/ARDS. Of note, reactivation of HSV-1 was predominantly observed in intubated patients regardless of their immune status, and a high HSV-1 DNA load in BALF was not associated with high-

Table 4. Laboratory and clinical findings of 14 patients diagnosed with or suspected of having viral pneumonia

Patient No.	Underlying disease	Virus	Diagnosis	DNA load		pp65 (+) cells	Other HHVs in BALF	Dominant CT finding	Antiviral agent	Outcome
				BAL copies/μg DNA	copies/ml blood					
1	SLE	CMV	proven	1.59×10^6	NA	82	none	GGO	ganciclovir	dead
2	posttransplant	CMV	proven	4.03×10^5	NA	206	EBV	GGO	ganciclovir	dead
3	SLE	CMV	proven	3.12×10^5	NA	34	EBV, HHV-7	GGO	ganciclovir	dead
4	MPA	CMV	proven	2.22×10^4	NA	0	none	GGO	ganciclovir	alive
5	DIHS	CMV	proven	1.39×10^4	NA	31	none	GGO	ganciclovir	dead
6	posttransplant	CMV	probable	5.65×10^5	NA	2	none	consolidation	ganciclovir	alive
7	SLE	CMV	probable	2.26×10^5	NA	30	none	GGO	ganciclovir	alive
8	DM-ILD	CMV	probable	5.70×10^3	NA	1	none	GGO	ganciclovir	dead
9	HIV-PCP	CMV	possible	1.70×10^5	NA	74	none	GGO	ganciclovir	alive
10	sepsis	HSV-1	possible	6.22×10^5	ND	NA	none	GGO	aciclovir	dead
11	posttransplant	HSV-1	possible	4.30×10^5	ND	0	none	GGO	none	dead
12	trauma	HSV-1	possible	2.00×10^5	NA	NA	none	GGO	aciclovir	dead
13	ML	HSV-1	possible	1.72×10^5	3.30×10^2	0	CMV	GGO	aciclovir	dead
14	posttransplant	HHV-6	probable	6.90×10^6	1.39×10^5	NA	none	GGO	foscarnet	dead

SLE = Systemic lupus erythematosus; MPA = microscopic polyangiitis; DIHS = drug-induced hypersensitivity syndrome; DM-ILD = dermatomyositis-associated interstitial lung disease; PCP = pneumocystis pneumonia; ML = malignant lymphoma; NA = not assessed; ND = not detected; GGO = ground-glass opacity.

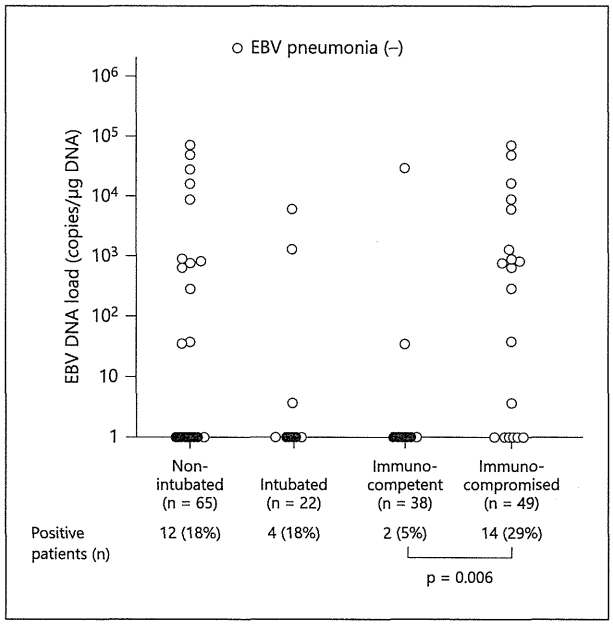

Fig. 3. EBV prevalence and semi-log plot of the EBV DNA load in BALF as a function of patient intubation or immune status. Negative PCR results were set to 1 ($\log_{10} 1 = 0$).

level viremia. These findings are in agreement with previous reports that HSV-1 pneumonia frequently presents as late-onset ventilator-associated pneumonia due to aspiration from the upper respiratory tract rather than pulmonary dissemination secondary to systemic viral infection [5, 6]. We also found that reactivation of HHVs other than HSV-1 mostly occurred in classically high-risk immunocompromised patients. Although recent studies have shown that CMV reactivation is common in nonimmunosuppressed, critically ill patients [8, 9], our results showed that CMV reactivation of the lung was rare in this patient population. Overall, clinically significant pulmonary reactivation of HHVs was almost exclusively observed in patients with endotracheal intubation or known immunocompromised status, indicating that patients with this clinical picture merit careful investigation for HHVs in the lung.

Viral pneumonia caused by HHVs still represents a diagnostic challenge. Demonstration of cytopathic effects by HHVs, indicating viral pathogenicity, is not a sensitive diagnostic tool and is often hard to obtain [23], while detection of HHVs via viral culture or PCR does not differentiate active infection from asymptomatic shedding. Therefore, combined use of real-time PCR with multiplex PCR is an integral part of the evaluation of HHV patho-

genicity. Since the amount of recovered epithelial lining fluid in BALF can vary considerably, the quantitative methodology in this study used data normalization to GAPDH, a housekeeping gene, to correct for this variation [24]. In agreement with previous studies [11–13], we found that quantification of the viral load in BALF may be useful in diagnosing CMV pneumonia. We noted that 3 patients with proven or probable CMV pneumonia had negative or clinically insignificant pp65 antigenemia, highlighting the importance of obtaining samples from the site of infection. Meanwhile, the pathogenicity of HSV-1 was unclear in this study because antiviral therapy did not lead to clinical improvement in 3 of 4 patients diagnosed with possible HSV-1 pneumonia. Previous studies also showed that HSV-1 in BALF may be a marker for underlying clinical conditions rather than a cause of mortality [25, 26]. In clinical practice, however, when there is a high viral load in BALF samples from ALI/ARDS of otherwise unexplained etiology, administration of antiviral agents against HHVs with possible lung pathogenicity (e.g. CMV, HSV-1, and HHV-6) would be an option for treatment.

We must acknowledge that it is difficult to extrapolate our results to all ALI/ARDS patients or to elucidate the etiologic role of HHVs in ALI/ARDS due to the selected group of patients and the retrospective nature of our study without a standardized diagnostic procedure. In addition, we must note that the pathogenic significance of HHVs is often difficult to determine via quantification of the viral DNA in BALF because of the substantial overlap between viral loads in symptomatic and asymptomatic patients [6, 11, 13]. Accordingly, although we have demonstrated that our diagnostic approach was technically feasible and potentially useful in ALI/ARDS patients to detect HHVs in the lung, further studies prospectively collecting all de novo ALI/ARDS patients in order to assess the exact prevalence of HHVs in ALI/ARDS or to investigate the possible impact of common bacterial infections on the reactivation of HHVs are needed. Also, a controlled antiviral treatment trial is warranted to draw conclusions regarding the etiologic role of the detected viruses in the development or worsening of ALI/ARDS.

Our study has some more limitations. First, there was a large heterogeneity in the studied population that precluded assessment of the impact of HHVs on the prognosis. Second, we may have underestimated the prevalence of HHVs because an HHV type with a low viral load in BALF could have been missed in the multiplex PCR assays if the BALF also contained a high viral load of another HHV type. Third, the impact of virus-bacteria coinfections could not be assessed because two thirds of our patients had received antimicrobial agents at the time of the BAL. Forth, oral contamination cannot be excluded because BALF samples obtained without a tracheal tube were possibly contaminated with oropharyngeal secretions by virtue of the technical procedure.

In conclusion, the implementation of multiplex and real-time PCR for HHVs allowed efficient detection and quantification of viral genomic DNA in BALF in selected ALI/ARDS patients of unknown etiology, especially in patients with immunosuppression or endotracheal intubation. In this setting, where clinicians must consider a wide differential diagnosis, the combination of multiplex and real-time PCR for HHVs may represent a useful diagnostic tool for the management of ALI/ARDS.

Acknowledgement

We thank Ms. Kyoko Maruyama, a medical technologist at the Institute of Biomedical Research and Innovation, for performing the PCR analysis. We also thank Drs. Takehiro Otoshi, Daichi Fujimoto, Takahisa Kawamura, Koji Tamai, Kazuya Monden, Takeshi Matsumoto, Jumpei Takeshita, and Kosuke Tanaka for performing BAL.

References

1 Rubenfeld GD, Herridge MS: Epidemiology and outcomes of acute lung injury. Chest 2007;131:554–562.

2 van der Bij W, Speich R: Management of cytomegalovirus infection and disease after solid-organ transplantation. Clin Infect Dis 2001;33:S32–S37.

3 Ramsey PG, Fife KH, Hackman RC, Meyers JD, Corey L: Herpes simplex virus pneumonia: clinical, virologic, and pathologic features in 20 patients. Ann Intern Med 1982;97:813–820.

4 Taplitz RA, Jordan MC: Pneumonia caused by herpesviruses in recipients of hematopoietic cell transplants. Semin Respir Infect 2002; 17:121–129.

5 Bruynseels P, Jorens PG, Demey HE, Goossens H, Pattyn SR, Elseviers MM, Weyler J, Bossaert LL, Mentens Y, Ieven M: Herpes simplex virus in the respiratory tract of critical care patients: a prospective study. Lancet 2003;362:1536–1541.

6 Luyt CE, Combes A, Deback C, Aubriot-Lorton MH, Nieszkowska A, Trouillet JL, Capron F, Agut H, Gibert C, Chastre J: Herpes simplex virus lung infection in patients undergoing prolonged mechanical ventilation. Am J Respir Crit Care Med 2007;175:935–942.

7 Linssen CF, Jacobs JA, Stelma FF, van Mook WN, Terporten P, Vink C, Drent M, Bruggeman CA, Smismans A: Herpes simplex virus load in bronchoalveolar lavage fluid is related to poor outcome in critically ill patients. Intensive Care Med 2008;34:2202–2209.

8 Limaye AP, Kirby KA, Rubenfeld GD, Leisenring WM, Bulger EM, Neff MJ, Gibran NS, Huang ML, Santo Hayes TK, Corey L, Boeckh M: Cytomegalovirus reactivation in critically ill immunocompetent patients. JAMA 2008; 300:413–422.
9 Chiche L, Forel JM, Roch A, Guervilly C, Pauly V, Allardet-Servent J, Gainnier M, Zandotti C, Papazian L: Active cytomegalovirus infection is common in mechanically ventilated medical intensive care unit patients. Crit Care Med 2009;37:1850–1857.
10 Mahony JB: Nucleic acid amplification-based diagnosis of respiratory virus infections. Expert Rev Anti Infect Ther 2008;8:1273–1292.
11 Zedtwitz-Liebenstein K, Jaksch P, Bauer C, Popow T, Klepetko W, Hofmann H, Puchhammer-Stockl E: Association of cytomegalovirus DNA concentration in epithelial lining fluid and symptomatic cytomegalovirus infection in lung transplant recipients. Transplantation 2004;77:1897–1899.
12 Chemaly RF, Yen-Lieberman B, Chapman J, Reilly A, Bekele BN, Gordon SM, Procop GW, Shrestha N, Isada CM, Decamp M, Avery RK: Clinical utility of cytomegalovirus viral load in bronchoalveolar lavage in lung transplant recipients. Am J Transplant 2005;5:544–548.
13 Bauer CC, Jaksch P, Aberle SW, Haber H, Lang G, Klepetko W, Hofmann H, Puchhammer-Stockl E: Relationship between cytomegalovirus DNA load in epithelial lining fluid and plasma of lung transplant recipients and analysis of coinfection with Epstein-Barr virus and human herpesvirus 6 in the lung compartment. J Clin Microbiol 2007;45:324–328.
14 Bernard GR, Artigas A, Brigham KL, Carlet J, Falke K, Hudson L, Lamy M, Legall JR, Morris A, Spragg R: The American-European Consensus Conference on ARDS: definitions, mechanisms, relevant outcomes, and clinical trial coordination. Am J Respir Crit Care Med 1994;149:818–824.
15 Sugita S, Iwanaga Y, Kawaguchi T, Futagami Y, Horie S, Usui T, Yamamoto S, Sugamoto Y, Mochizuki M, Shimizu N, Watanabe K, Mizukami M, Morio T: Detection of herpesvirus genome by multiplex polymerase chain reaction (PCR) and real-time PCR in ocular fluids of patients with acute retinal necrosis (in Japanese). Nippon Ganka Gakkai zasshi 2008;112:30–38.
16 Sugita S, Shimizu N, Watanabe K, Mizukami M, Morio T, Sugamoto Y, Mochizuki M: Use of multiplex PCR and real-time PCR to detect human herpes virus genome in ocular fluids of patients with uveitis. Br J Opthalmol 2008; 92:928–932.
17 Brodoefel H, Vogel M, Spira D, Faul C, Beck R, Claussen CD, Horger M: Herpes-simplex-virus 1 pneumonia in the immunocompromised host: high-resolution CT patterns in correlation to outcome and follow-up. Euro J Radiol 2012;81:e415–e420.
18 Feldman S: Varicella-zoster virus pneumonitis. Chest 1994;106:22S–27S.
19 Liu QF, Fan ZP, Luo XD, Sun J, Zhang Y, Ding YQ: Epstein-Barr virus-associated pneumonia in patients with post-transplant lymphoproliferative disease after hematopoietic stem cell transplantation. Transpl Infect Dis 2010; 12:284–291.
20 Carrigan DR, Drobyski WR, Russler SK, Tapper MA, Knox KK, Ash RC: Interstitial pneumonitis associated with human herpesvirus-6 infection after marrow transplantation. Lancet 1991;338:147–149.
21 Sauter A, Ernemann U, Beck R, Klingel K, Mahrholdt H, Bitzer M, Horger M: Spectrum of imaging findings in immunocompromised patients with HHV-6 infection. AJR Am J Roentgenol 2009;193:W373–W380.
22 Franquet T: Imaging of pulmonary viral pneumonia. Radiology 2011;260:18–39.
23 Crawford SW, Bowden RA, Hackman RC, Gleaves CA, Meyers JD, Clark JG: Rapid detection of cytomegalovirus pulmonary infection by bronchoalveolar lavage and centrifugation culture. Ann Intern Med 1988;108: 180–185.
24 Kriegova E, Arakelyan A, Fillerova R, Zatloukal J, Mrazek F, Navratilova Z, Kolek V, du Bois RM, Petrek M: PSMB2 and RPL32 are suitable denominators to normalize gene expression profiles in bronchoalveolar cells. BMC Mol Biol 2008;9:69.
25 Scheithauer S, Manemann AK, Kruger S, Hausler M, Kruttgen A, Lemmen SW, Ritter K, Kleines M: Impact of herpes simplex virus detection in respiratory specimens of patients with suspected viral pneumonia. Infection 2010;38:401–405.
26 Bouza E, Giannella M, Torres MV, Catalan P, Sanchez-Carrillo C, Hernandez RI, Munoz P: Herpes simplex virus: a marker of severity in bacterial ventilator-associated pneumonia. J Crit Care 2011;26:432.e431–e436.

INTERNAL MEDICINE

ORIGINAL ARTICLE

Analysis of Viral Infection by Multiplex Polymerase Chain Reaction Assays in Patients with Liver Dysfunction

Kiminari Ito[1], Norio Shimizu[2], Ken Watanabe[2], Toshiharu Saito[3], Yuriko Yoshioka[3], Emiko Sakane[1], Hiroko Tsunemine[1], Hiroshi Akasaka[1], Taiichi Kodaka[1] and Takayuki Takahashi[1]

Abstract

Objective While unexplained liver dysfunction is common, it is sometimes difficult to identify its exact cause. One cause is viral infections. The identification of viruses other than hepatitis B and C that cause liver dysfunction is difficult because no methods to simultaneously identify these viruses have been established. The aim of this study was to quickly and simultaneously identify multiple virus species.

Methods A total of 49 patients with unexplained liver dysfunction and undetermined inflammation were examined. The majority of patients had hematologic malignancies, and some had undergone bone marrow transplantation. Qualitative polymerase chain reactions (PCR) were performed to detect 12 species of DNA virus in whole blood. Quantitative real-time PCR was performed when a specific virus was amplified. In addition, 6 RNA hepatitis viruses were directly assayed by real-time PCR. These 2 PCR steps were completed within 1 hour.

Results The most frequently detected virus in 37 patients with liver dysfunction, was transfusion transmitted virus (38%), which was followed by human herpes virus (HHV) type 6 (35%), Epstein-Barr virus (14%), cytomegalovirus (8%), and rarely hepatitis G virus and HHV-7 (3%). Similar viremia was observed in 12 patients with mild liver dysfunction. The results of the PCR assay were mostly consistent with those of routine virus serological tests.

Conclusion A multiplex viral PCR assay was a useful tool for quickly identifying viruses that possibly cause liver dysfunction. It was also important that liver dysfunction acted as a proband that led to the discovery of serious viremia.

Key words: liver dysfunction, multiplex PCR, real-time PCR, human herpes viruses, hepatitis virus

(Intern Med 52: 201-211, 2013)
(DOI: 10.2169/internalmedicine.52.8206)

Introduction

A clinician often encounters unexplained liver dysfunction; however, it is sometimes difficult to identify the exact cause of the dysfunction because of the many causes of liver dysfunction. One common cause of liver dysfunction is viral infection. Although it is easy to detect hepatitis B virus (HBV) and hepatitis C virus (HCV) because of the established laboratory tests for these viruses, the detection of other viruses that cause liver dysfunction is difficult because the current laboratory methodologies in a hospital have some limitations in terms of quick performance and the limited number of identifiable viral species. Therefore, the prompt and proper diagnosis of viral infections is important when a patient exhibits liver dysfunction. An assay was developed to simultaneously detect 12 kinds of viral DNA genomes in the blood. The assay uses a multiplex polymerase chain reaction (PCR) to identify the viruses, and real-time PCR to determine the viral load. In addition, 6 RNA

[1]Department of Hematology, Shinko Hospital, Japan, [2]Department of Virology, Medical Research Institute, Tokyo Medical and Dental University, Japan and [3]Laboratory of Cell Therapy, Shinko Hospital, Japan
Received for publication May 21, 2012; Accepted for publication September 12, 2012
Correspondence to Dr. Takayuki Takahashi, takahashi.takayuki@shinkohp.or.jp

Table 1. Primer and Probe Sequences Employed in Multiplex Qualitative Polymerase Chain Reaction (PCR) Analyses

Virus	Region of amplification	Primer sequence	Probe sequence	Reference
HSV1/HSV-2	polymerase	F: GCTCGAGTGCGAAAAAACGTTC	3'FITC: GCGCACCAGATCCACGCCCTTGATGAGC	3
		R: TGCGGTTGATAAACGCGCAGT	LcRed604-5': CTTGCCCCCGCAGATGACGCC	
VZV	gene29	F: TGTCCTAGAGGAGGTTTTATCTG	3'FITC: GGGAAATCGAGAAACCACCCTATCCGAC	4
		R: CATCGTCTGTAAAGACTTAACCAG	LcRed640-5': AAGTTCGCGGTATAATTGTCAGT	
EBV	BamH1	F: CGCATAATGGCGGACCTAG	3'FITC: AAAGATAGCAGCAGCGCAGC	GeneBank V01555
		R: CAAACAAGCCCACTCCCC	LcRed640-5': AACCATAGACCCGCTTCCTG	
CMV	Glycoprotein	F: TACCCCTATCGCGTGTGTTC	3'FITC: TCGTCGTAGCTACGCTTACAT	5
		R: ATAGGAGGCGCCACGTATTC	LcRed705-5': ACACCACTTATCTGCTGGGCAGC	
HHV6	101k gene region	F: ACCCGAGAGATGATTTTGCG	3'FITC: TAAGTAACCGTTTTCGTCCCA	6
		R: GCAGAAGACAGCAGCGAGAT	LcRed705-5': GGGTCATTTATGTTATAGA	
HHV7	U57	F: GAAAAATCCGCCATAATAGC	3'FITC: GCCATAAGAAACAGGTACAGACATTGTCA	GeneBank NC001716
		R: ATGGAACACCTATTAACGGC	LcRed705-5': TTGTGAAATGTGTTGCG	
HHV8	EB BDLF1ORF21	F: AGCCGAAAGGATTCCACCAT	3'FITC: CCGGATGATGTAAATATGGCGGAAC	7
		R: TCCGTGTTGTCTACGTCCAG	LcRed705-5': TGATCTATATACCACCAATGTGTCATTTATG	
BKV/JCV	VP2	F: CACTTTTGGGGGACCTAGT	3'FITC: TCTGAGGCTGCTGCTGCCACAGGATTTT	8
		R: CTCTACAGTAGCAAGGGATGC	LcRed705-5': AGTAGCTGAAATTGCTGCTGGAGAGGCTGCT	
Parvo B19	NS1	F: CCGCCAAGTACAGGAAAAAC	3'FITC: GCAAAAGCCATTTTAGGCGGGCA	9
		R: CAGCTACACTTCCACGCA	LcRed640-5': CACCAGGGTAGATCAAAAAATGCGTGGA	

BKV/JCV: BK virus/JC virus, CMV: cytomegalovirus, F: Forward, FITC: Fluorescein isothiocyanate, EBV: Epstein-Barr virus, HHV: human herpes virus, HSV: herpes simplex virus, Parvo B19: Parvovirus B19, R: Reverse, VZV: varicella-zoster virus

hepatitis viruses were directly quantified with real-time PCR. Our multiplex PCR combined with real-time PCR was highly useful in the quick diagnosis of viral hepatitis.

Materials and Methods

Patients

Patients with unexplained liver dysfunction, that received medical care in Shinko Hospital, Kobe, Japan, from February to December, 2011 were enrolled in this study. Liver dysfunction in this study was defined as patients that exhibited more than 2 times the normal upper limits of aspartate transaminase (AST) (80 IU/L), alanine transaminase (ALT) (80 IU/L), or alkaline phosphatase (ALP) (720 IU/L) levels or more than 1.5 mg/dL of total bilirubin, with negative serological tests for HBsAg and HCV. Patients with normal liver function or mild dysfunction underwent this viral PCR examination for possible viral infection because of fever or inflammatory signs. These patients were enrolled in this study. Patients who showed positive results for HBV or HCV by serological or molecular examinations were also included in this study in order to examine the possibilility of multiple viral loads. In addition, the serological tests for both HBV and HCV were performed before the multiplex PCR analysis in all patients included in this study.

Blood and plasma samples

EDTA-2Na-chelated whole blood (200 μL) was obtained from individual patients who provided their written informed consent. The present study was part of a retrospective analysis of a single institutional clinical study designated the "Multiple Virus-Analytic Study by Multiplex PCR", which had been approved by the institutional review board. The plasma was separated from whole blood by centrifugation at 400-g when 1 or more virus-specific PCR products/signals were detected, and subjected to real-time PCR in order to quantify the number copies of the viral genome. Blood obtained from 12 healthy volunteers with informed consent was subjected to the following virus analyses as negative controls.

Multiplex PCR (1, 2)

DNA was extracted from the whole blood using QuickGene DNA whole blood kit S (FUJIFILM Corporation, Tokyo, Japan) that was installed on an apparatus for the automated purification of nucleic acids (QuickGene-800; FUJIFILM Corporation). The multiplex PCR was designed to qualitatively measure the genomic DNA of 12 viruses; cytomegalovirus (CMV), human herpes virus type 6 (HHV-6), Epstein-Barr virus (EBV), varicella-zoster virus (VZV), BK virus (BKV), JC virus (JCV), parvovirus B19 (ParvoB19), human herpes virus type 7 (HHV-7), human herpes virus type 8 (HHV-8), herpes simplex virus type 1 (HSV-1) and type 2 (HSV-2), and HBV.

The PCR was performed using a LightCycler (Roche, Basel, Switzerland). The primers and probe sequences for these 12 viruses are described in Table 1 (3-9).

Two sets were paired-off with the following capillaries of these 12 viruses; Capillary A: HSV-1, HSV-2, VZV, HHV-6, CMV, Parvo B19, BKV, and JCV, and Capillary B: EBV, HHV-7, and HHV-8. Specific primers for these viruses were used with 0.25 μL AccuPrime Taq polymerase and 1× AccuPrime Buffer I (Invitrogen Corporation, Carlsbad, CA, USA) and 5 ng non-acetylated bovine serum albumin (BSA; Sigma-Aldrich Co., St. Louis, MO, USA), resulting in a final volume of 10 μL for each primer. First, 3 μL of mineral oil (Sigma-Aldrich Co.) was placed in the capillary. Next, 10 μL of reaction mixture was added and centrifuged for 3,000 rpm for 3 s. Finally, 5 μL of probe mix was added to the capillary, which was then capped. The DNA was amplified with 40 PCR cycles at 95℃ (2 s), 58℃ (15 s), and 72℃ (15 s), which was followed by denaturation at 95℃ (1 min).

Fluorescein isothiocyanate-conjugated probe hybridization and LCRed640- or LCRed-conjugated hybridization probes were then mixed with the products by 3,000 rpm centrifugation for 3 s. Specific hybridization was confirmed by a melting curve analysis (10) in which the dissociation of hybridized probes from individual PCR products was seen as the

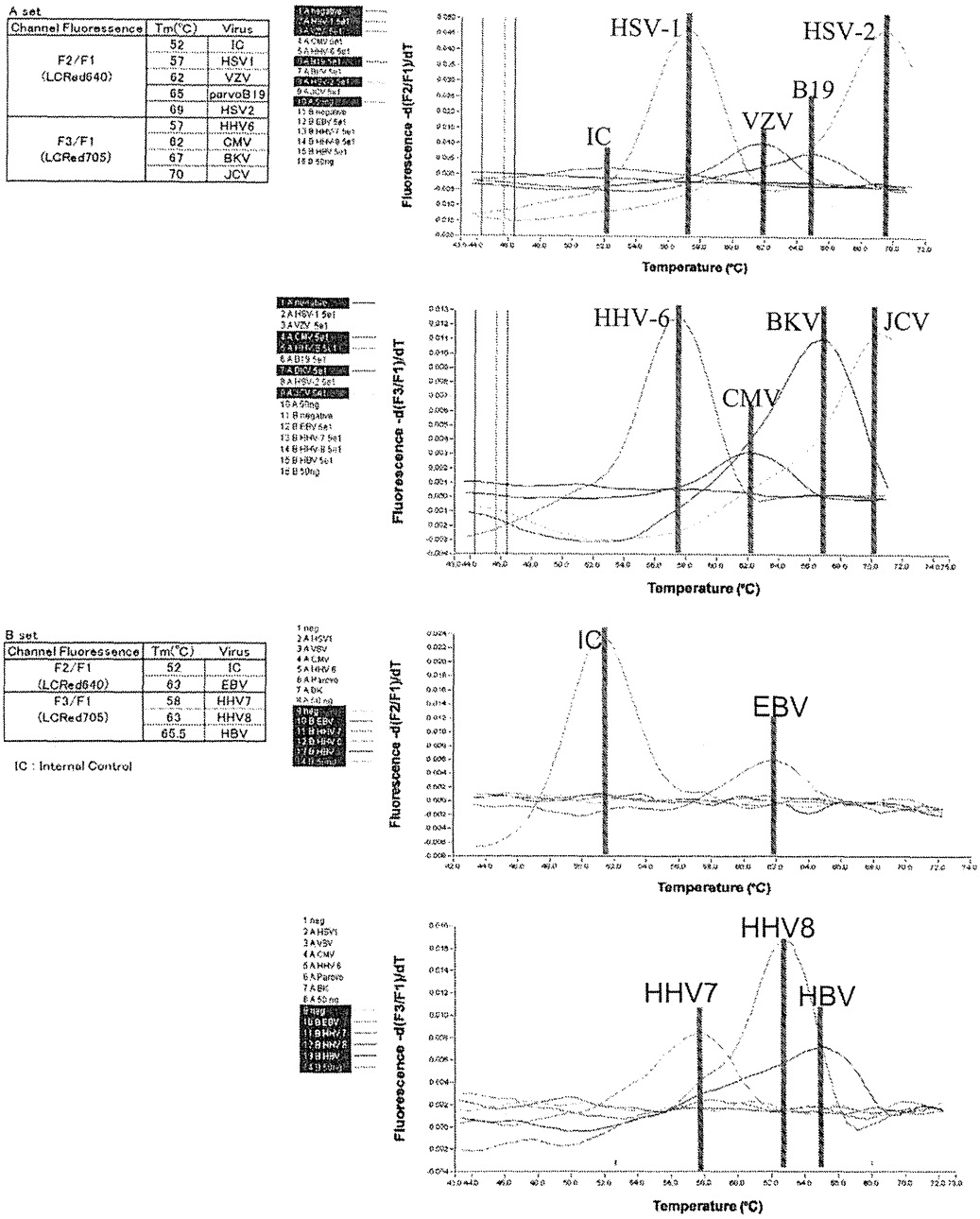

Figure. Melting curve analysis by virus-specific melting temperature (Tm). A melting curve analysis is used to measure the temperature at which the DNA is split into single chain from double stranded DNA. The PCR products amplified by the primer for each viral sequence hybridize the specific probes labeled by LcRED705 and LcRED640 at 40°C. This hybridized double strand DNA melted/dissociated when it was heated gradually from 40°C to 80°C. Each viral melting temperature was measured by use of the fluorescence resonance energy transfer (FRET). Releasing the excitation energy causes the fluorescent substance that reached the excitation state to return to the basal state, and that neighboring fluorescent substance obtains the energy and enters into the excitation state. The melting temperature of individual DNA strands is determined based on each viral sequence, the length, and the GC content. BKV/JCV: BK virus/JC virus, CMV: cytomegalovirus, HHV: human herpes virus, HSV: herpes simplex virus, IC: immune complexed, B19: Parvovirus B19, VZV: varicella-zoster virus

disappearance of fluorescence at the specific dissociation temperature of each virus. The specific temperature for each virus is shown in Figure. The melting curve analysis was performed by denaturing DNA at 95℃ for 1 minute, which was followed by hybridization at 40℃ for 10 s and melting at 40℃ to 80℃ (Ramp rate, 0.2℃/s).

In addition, a sensitivity test of this PCR was performed using known plasmid DNA representatives for the 12 individual DNA viruses. The individual DNA sequences were determined based on the database for DNA viruses, and the

Table 2. Sensitivity of Qulitative Multiplex PCR

	Copies / Tube				
	100	50	25	10	Sensitivity
HSV1	10/10	10/10	10/10	7/10	>25 copies
HSV2	10/10	10/10	10/10	10/10	>10 copies
VZV	10/10	10/10	10/10	10/10	>10 copies
CMV	10/10	10/10	10/10	10/10	>10 copies
EBV	10/10	10/10	10/10	9/10	>25 copies
HHV6	10/10	10/10	10/10	8/10	>25 copies
HHV7	10/10	10/10	5/10	4/10	>50 copies
HHV8	10/10	10/10	6/10	5/10	>50 copies
BKV	10/10	10/10	10/10	10/10	>10 copies
JCV	10/10	10/10	9/10	7/10	>50 copies
HBV	10/10	10/10	6/10	1/10	>50 copies
ParvoB19	10/10	10/10	10/10	10/10	>10 copiee

HSV: herpes simplex virus, VZV: varicella-zoster virus, CMV: cytomegalovirus, EBV: Epstein-Barr virus,
HHV: human herpes virus, BKV: BK virus, JCV: JC virus, HBV: hepatitis B virus, ParvoB19: Parvovirus B19

plasmid DNAs were synthesized by Nihon Techno Service Company, Ibaragi, Japan. The qualitative PCR assay was performed 10 times for each virus using various concentrations of the plasmid DNA and determined the concentration of the plasmid DNA (copy number/tube) as the detection limit when 100% positivity (10/10 assays) was obtained. Table 2 shows that the sensitivity of the PCR varied from more than 10 to 50 copies.

The assay could directly measure the load with a linear relationship up to 10^9 copies/tube; however, dilution was required when the viral load exceeded 10^{10} copies.

Real-time PCR (1, 2)

Real-time PCR was performed when a positive and specific result was obtained by multiplex PCR for the human herpes viruses. Quantitative reverse transcription (RT)-PCR was performed first for the human RNA hepatitis viruses. Hepatitis A virus (HAV), hepatitis B virus (HBV), hepatitis C virus (HCV), hepatitis D virus (HDV), hepatitis E virus (HEV), hepatitis G virus (HGV), and transfusion transmitted virus (TTV) we assayed as the infecting organisms of a human hepatitis virus. Real-time PCR was performed using 0.5 Units of Taq DNA polymerase (Thermo Fished Scientific Inc., Waltham, MA, USA), 1 mM dNTPs (Bioline USA Inc., Taunton, MA, USA), 3 mM $MgCl_2$ (NIPPON GENE Co. Ltd., Tokyo, Japan), 0.1 μg Anti-taq high (Toyobo Co. Ltd., Osaka, Japan), 10 ng non-acetylated BSA (Sigma-Aldrich Co.), and One Step PrimeScript Real-time RT-PCR kits (Takara Bio Inc., Shiga, Japan). Each reaction final volume was 20 μL, and the reaction was performed on the Light Cycler DX400 (Roche).

The sequence for the primers and the probes of each virus are shown in Table 3A, B (11-21). The DNA of human herpes virus and HBV were amplified by PCR with the following conditions: denaturation at 95℃ (10 s) and then 50 cycles of PCR (denaturation at 95℃ [1 s], annealing at 60℃ [20 s], and cooling at 40℃ [20 s]). The RNA of the remaining hepatitis viruses was amplified by RT-PCR with following conditions: RT reaction at 42℃ (5 min), denaturation at 95℃ (10 s), 50 cycles of PCR (denaturation at 95℃ [1 s], annealing at 60℃ [20 s], and cooling at 40℃ [20 s]. The value of the viral-genome copy number in the sample was considered to be significant when more than 10 copies/tube were obtained.

The real-time PCR was repeated 8 times on a VZV-positive specimen that contained 10 copies/tube of VZV plasmid. The mean value of cycle numbers required to obtain 10 copies/tube were 28. 28 cycles with a standard deviation (SD) of 0.317 cycles. The distribution coefficient was 0.393, indicating excellent reproducibility of this quantitative PCR. Each cycle number for the reproducibility was tested with the Kolmogov-Smirnov test assuming as normal distribution.

These multiplex PCR and real-time PCR procedures of the present study were performed in the Laboratory of Cell Therapy in Shinko Hospital.

Results

Viruses identified in patients with unexplained liver dysfunction

A total of 49 patients were included in this study. The characteristics and the laboratory data of these patients with unexplained liver dysfunction are described in Tables 4, 6. The majority of the patients had hematologic malignancies and were immune-compromised, especially, those patients who were seen soon after allogeneic bone marrow transplantations. One or more viral species was detected in 28 of the 37 patients with liver dysfunction, and their copy number was determined (Table 4). The most frequently detected virus was TTV (14/37), which was followed by HHV-6 (13/37), EBV (5/37), CMV (3/37), and rarely HGV (1/37) and HHV-7(1/37). Three virus species were detected in 2 patients (Nos. 32 and 36); 2 species were detected in 8 patients; and a single virus was detected in 19 remaining patients. However, no virus genomes were detected in 9 of the 37 patients, indicating that there were other causes of liver dysfunction in these patients at the time of the analysis. One patient that was diagnosed with chronic hepatitis B (No. 36) was infected with both EBV and TTV in addition to HBV, suggesting that co-viral infections may exists in patients with hepatitis B. The incidence of fever or skin rash in this cohort of patients was low (Table 4) presumably due to the immunosuppressive procedures or chemotherapies in the majority of these patients.

Twelve healthy volunteers were examined in the same way as a negative control. Table 4 shows that none of the 12 DNA viruses were detected by the multiplex PCR in these volunteers. As for hepatitis viruses, all 7 hepatitis viruses except TTV were below the detection limit. TTV was detected in 2 of 12 volunteers with a viral load ranging from 5×10^1 to 7.7×10^2 copies/mL (Table 4).

Table 3A. Primer and Probe Sequences in the Assay of Human Herpes Virus (HHV) by Reverse Transcriptase-polymerase Chain Reaction

Herpes virus	Primers and probe sequences	Amplification	Referance
HSV1 and 2	HSV-F: CGCATCAAGACCACCTCCTC	gB	11
	HSV-R: GCTCGCACCACGCGA		
	HSV1-P: JOE-TGGCAACGCGGCCCAAC-TAMRA		
	HSV2-P: FAM-CGGCGATGCGCCCCAG-TAMRA		
VZV	VZV-F: AACTTTTACATCCAGCCTGGCG	ORF29	GeneBankX04370,AJ871403,DQ457052
	VZV-R: GAAAACCCAAACCGTTCTCGAG		
	VZV-P: FAM-TGTCTTTCACGGAGGCAAACACGT-TAMRA		
EBV	EBV-F: CGGAAGCCCTCTGGACTTC	BALF-5	12
	EBV-R: CCCTGTTTATCCGATGGAATG		
	EBV-P: FAM-TGTACACGCACGAGAAATGCGCC-TAMRA		
CMV	CMV-F: CATGAAGGTCTTTGCCCAGTAC	U65-U66	13
	CMV-R: GGCCAAAGTGTAGGCTACAATAG		
	CMC-P: FAM-TGGCCCGTAGGTCATCCACACTAGG-TAMRA		
HHV6	HHV6-F: GACAATCACATGCCTGGATAATG	U37	14
	HHV6-R: TGTAAGCGTGTGGTAATGTACTAA		
	HHV6-P: FAM-AGCAGCTGGCGAAAAGTGCTGTGC-TAMRA		
HHV7	HHV7-F: CGGAAGTCACTGGAGTAATGACAA	U57	15
	HHV7-R: CCAATCCTTCCGAAACCGAT		
	HHV7-P: FAM-CTCGCAGATTGCTTGTTGGCCATG-TAMRA		
HHV8	HHV8-F: CCTCTGGTCCCCATTCATTG	ORF65	16
	HHV8-R: CGTTTCCGTCGTGGATGAG		
	HHV8-P: FAM-CCGGCGTCAGACATTCTCACAACC-TAMRA		
BKV/JCV	BKV & JCVF: GGAAAGTCTTTAGGGTCTTCTACCTTT	ORF	17
	BKV-R: GATGAAGATTTATTYTGCCATGARG		
	JCV-R: GAAGACCTGTTTTGCCATGAAGA		
	BKV & JCV-P: 6FAM-ATCACTGGCAAACAT-MGB		
Parvob19	B19-F: GGGTTTCAAGCACAAGYAGTAAAAGA	NS1	GeneBank M13178,AJ717293,AX003421
	B19-R: CGGYAAACTTCCTTGAAAATG		
	B19-P: FAM-CAGCTGCCCCTGTGG-MGB		

The real-time herpes simplex virus (HSV) PCR is a multiplex PCR that can detect both HSV1 and HSV2 DNA in the same reaction. The optimized gB primer pairs amplify both HSV1 and 2 with equal efficiency, with the 2 type-specific probes labeled with different fluorescent dyes. The HSV1 probe is labeled with JOE at the 5'-end and with TAMRA at the 3'-end. The HSV2 probe is labeled with FAM at the 5'-end and with TAMRA at the 3'-end.
CMV: cytomegalovirus, EBV: Epstein-Barr virus, VZV: Varicella-zoster virus

Table 3B. Primer and Probe Sequences in the Assay of Human Hepatitis Virus by Reverse Transcriptase-polymerase Chain Reaction

	Primer and Probe Sequences	Amplification	Reference
HAV	HAV-F:GGTAGGCTACGGGTGAAACC	5'NC	GeneBank :AB020564、AB020565,
	HAV-R:GCCGCTGTTACCCTATCCAA		AB020568,AB020568,M14707,K02990,
	HAV-P:FAM-TACTTCTATGAAGAGATGC-MGB		X75216,X75215
HBV	HBV-F:GTGGTGGACTTCTCTCAATTTTCTAG	S-gene	
	HBV-R:GGACAMACGGGCAACATACCT		AF090842,AF100309,,X04615
	HBV-P:FAM-TGTCTGCGGCGTTTT		
HCV	GTCTAGCCATGGCGTTAGTA	57NC	GeneBank:
	CTCGCAAGCACCCTATCAGGCAGT		AF009606,AF356827,D14853,AF169004,
	HCV-P:FAM-CTGCGGAACCGGTGAGTACAC-BHQ		AB030907,D50409,D17763
HDV	HDV-F:GCATGGTCCCAGCCTCC	ribozyme I	
	HDV-R:TCTTCGGGTCGGCATGG		18
	HDV-P:FAM- ATGCCCLaGGLtCGGAC-TAMRA		
HEV	HEV-F:GGTGGTTTCTGGGGTGAC	ORF3	
	HEV-R:AGGGGTTGGTTGGATGAA		19
	HEV-P:FAM- TGATTCTCAGCCCTTCGC -TAMRA		
HGV	HGV-F:CGGCCAAAAGGTGGTGGATG	5'NC	
	HGV-R:CGG TAGGGCCAACACCTGTGGA		20
	HGV-P:FAM- CAGGGTTGGTAGGTCGTAAATCCCGGTCA-TAMRA		
TTV	TTV-F:TCCGAATGGCTGAGTTT	ORF2	
	TTV-R:CGAATTGCCCCTTGACT		21
	TTV-P:FAM- ACTCACCTHCGGCACCCGC-iowaBK		

HAV: hepatitis A virus, HBV: hepatitis B virus, HCV: hepatitis C virus, HDV: hepatitis D virus, HEV: hepatitis E virus, HGV: hepatitis G virus, TTV: transfusion transmitted virus

Follow-up examination of liver dysfunction and viremia

The study then examined the relationship between the liver dysfunction and viremia. The detected viruses were re-examined after appropriate intervals in 15 of the 37 patients included in the present study. Table 5 shows that the liver dysfunction was improved or normalized in almost all patients reexamined. The load of HHV-6 virus decreased with the improvement of the liver dysfunction in all 6 patients re-examined for this virus. The correlation between the copy number of HHV-6 and the levels of AST, ALT, and ALP was analyzed at 2 periods of the examination using Restricted Maximum Likelihood. The improvement of the

Table 4. Characteristics of Patients with Unexplained Liver Dysfunction and Their Laboratory Data

Patient No.	Age	Sex	Underlying disease	AST	ALT	ALP	T.Bil	LDH	CRP	% of Atyp. lym	Fever	Skin rash	LN swelling	History of transfusion	Virus detected and its copy number
1	82	M	Pulmonary Tbc	67	156	375	0.7	218	1.45	0	±	−	−	None	None
2	65	M	IP	32	95	319	0.8	288	1.40	0	±	−	−	None	None
3	36	F	Septic shock	96	50	802	10.0	489	11.80	1.6	+	−	−	None	HHV-6: 3.9×10^3
4	69	F	ATL post BMT	168	190	241	0.8	356	0.24	0	−	−	−	None	HHV-6: 8.3×10^2
5	36	M	post HPS	56	138	306	0.5	324	0.07	8.0	−	−	−	None	None
6	49	M	Malignant lymphoma	49	110	333	1.0	254	0.71	0.5	−	−	−	RCC	HHV-6: 4.7×10^2
7	70	M	FUO	43	72	1,678	0.7	121	16.93	0	+	−	−	None	None
8	72	F	MDS/AML	119	64	465	0.7	259	0.39	1.6	−	−	−	RCC, PC	HGV: 1.8×10^6
9	53	M	AML, post BMT	39	99	711	0.4	114	0.28	0.4	−	+	−	RCC, PC	HHV-6: 6.1×10^3
10	78	F	Myeloma, Pneumonia	54	117	183	1.7	689	1.97	1.0	±	−	−	RCC, PC	CMV: 3.6×10^4, EBV: 8.0×10^2
11	85	M	MDS	470	215	968	1.9	647	0.11	0	−	−	−	None	TTV: 5.1×10^3
12	66	F	Multiple myeloma	45	80	1,059	1.0	335	18.70	32.4	+	−	−	RCC, PC	None
13	56	M	MDS post BMT	93	93	228	0.8	493	3.45	0.8	+	−	−	RCC, PC	None
14	59	M	Malignant lymphoma	158	326	644	1.3	274	2.12	1.5	±	−	−	None	HHV-6: 1.7×10^2, TTV: 1.2×10^4
15	34	F	ALL	448	481	1,420	2.0	719	12.54	0	+	−	−	RCC, PC	TTV: 1.2×10^5
16	62	M	Malignant lymphoma	137	197	973	2.1	407	7.91	0.5	+	−	−	RCC, PC	None
17	75	F	Drug-induced hepatitis	124	361	526	1.2	185	0.19	0	−	−	−	None	HHV-6: 1.6×10^3
18	36	F	Infectious mononucleosis	511	469	411	0.6	675	0.65	33.5	±	−	+	None	CMV: 1.7×10^4
19	44	F	Infectious mononucleosis	169	352	1,956	1.4	393	0.65	38.9	±	−	+	None	EBV: 1.1×10^5
20	66	F	Autoimmune hepatitis	418	645	602	0.8	329	0.27	0	−	−	−	None	TTV: 5.8×10^3
21	25	F	Infectious mononucleosis	87	114	354	0.9	450	0.91	38.3	+	+	+	None	CMV: 5.7×10^4, HHV-6: 3.6×10^2
22	67	F	ATL	1,189	1,186	2,900	0.5	796	7.66	21.8	+	+	−	RCC, PC	HHV-6: 1.0×10^5
23	65	F	IP	66	76	721	0.5	712	18.98	0	+	−	−	None	None
24	86	M	Malignant lymphoma	481	433	1,182	0.6	576	0.03	0	−	−	−	None	HHV-6: 7.0×10^3, EBV: 6.4×10^2
25	54	M	AIDS	84	43	1,130	0.3	262	1.15	0	±	−	+	None	HHV-6: 1.5×10^3, EBV: 7.1×10^2
26	73	F	Myeloma	241	486	222	2.1	567	3.61	0.5	±	−	−	RCC, PC	HHV-6: 1.7×10^3, TTV: 4.1×10^2
27	70	M	Knee joint MRSA infection	21	29	683	0.9	141	1.89	1.0	±	−	−	None	TTV: 3.5×10^4
28	57	F	Sepsis	158	37	387	0.4	625	33.80	0	+	−	−	None	None
29	50	M	PH	42	84	497	0.2	264	1.85	0	−	−	−	None	TTV: 4.5×10^4
30	50	F	AML	20	86	179	0.3	148	0.06	0	−	−	−	RCC, PC	TTV: 9.0×10^3
31	32	F	AML, post BMT	173	230	275	0.5	193	0.19	2.4	−	−	−	RCC, PC	TTV: 4.4×10^6
32	52	M	ALL, post BMT	26	58	663	0.7	214	15.31	1.2	+	±	−	RCC, PC	HHV-6: 1.2×10^4, HHV-7: 7.7×10^3, TTV: 4.9×10^3
33	44	F	MDS, post BMT	36	84	209	0.9	239	0.17	0.8	−	−	−	RCC, PC	HHV-6: 1.9×10^4, TTV: 2.7×10^5
34	19	M	Malignant lymphoma	48	125	181	0.7	161	0.26	0	−	−	±	None	TTV: 5.5×10^2
35	76	F	Drug-induced hepatitis	578	384	920	2.1	562	0.39	0	−	−	−	None	TTV: 7.3×10^3
36	80	M	Hepatitis B (chronic)	1,502	868	459	3.8	427	1.32	0.4	±	−	−	None	HBV:1.6×10^8, EBV: 1.5×10^3, TTV: 7.8×10^4
37	57	M	Hepatitis B (acute)	938	1,707	917	3.3	459	1.15	0	±	−	−	None	HBV: 1.5×10^8
12 Healthy volunteers				HHV-1,2, VZV, EBV, CMV, HHV-6,7,8, BKV, JCV, PalvoB19: N.D.										HAV, HBV, HCV, HDV, HEV, HGV: <10 copies.	
														TTV: positive in 2 of 12; 5×10^1–7.7×10^2 copies.	

Normal upper limits of AST, ALT, ALP, T-Bil, LDH, and CRP are 40 IU/L, 40 IU/L, 360 IU/L, 1.3 mg/dL, 230 IU/L, and 0.3 mg/dL, respectively. The copy number of each virus listed is expressed in its copy number /mL.

Atyp. Lym: atypical lymphocyte, PC: platelet concentrate, RCC: red cell concentrate, AIDS: acquired immunodeficiency syndrome, ALL: acute lymphoblastic leukemia, ALP: alkaline phosphatase, ALT: alkaline transaminase, AML: acute myeloid leukemia, ATL: adult T-cell leukemia, BMT: bone marrow transplantation, CRP: C-reactive protein, FUO: fever of unknown origin, HPS: hemophagocytic syndrome, IP: interstitial pneumonia, LDH: lactate dehydrogenase, LN: lymph node, MDS: myelodysplastic syndrome, PH: pulmonary hypertension, Tbc: tuberculosis, T.Bil: total bilirubin, MRSA: methicillin-resistant Staphylococcus aureus, N.D: not detected

Intern Med 52: 201-211, 2013 DOI: 10.2169/internalmedicine.52.8206

Table 5. Patients Reexamined for Liver Dysfunction and Previously Documented Viremia

Patient No.	Age	Sex	Time of reexamination	AST	ALT	ALP	T.Bil	LDH	CRP	Fever	Skin rash	LN swelling	Virus detected and its copy number
3	36	F	after 8 M	29	11	337	0.3	420	3.76	±	−	−	HHV-6: not detectable
4	69	F	after 4 M	34	34	186	0.8	272	0.14	−	−	−	HHV-6: 4.3×10^1
6	49	M	after 4 M	37	70	347	0.4	207	0.06	−	−	−	HHV-6: 1.0×10^1
8	72	F	after 6 M	48	19	289	0.8	227	2.11	−	−	−	HGV: 5.3×10^4
9	53	M	after 4 M	19	28	465	0.5	197	0.03	−	−	−	HHV-6: 1.0×10^3
11	85	M	after 2 W	615	670	1,739	2.0	649	0.24	−	−	−	TTV: 3.5×10^3
18	36	F	after 6 days	152	278	430	0.7	417	0.38	±	−	+	CMV: not reexamined
19	44	F	after 9 days	140	344	1,062	0.8	246	0.05	±	−	±	EBV: not reexamined
20	66	F	after 2 M	17	26	139	0.4	147	3.13	−	−	−	TTV: 9.0×10^3
21	25	F	after 2 M	21	12	221	0.5	161	0.02	−	−	±	CMV:undetectable, HHV-6: not detectable
22	67	F	after 3 M	26	6	278	0.9	328	5.43	−	−	−	HHV-6: 1.4×10^3
27	70	M	after 2 W	78	72	494	2.9	257	2.34	±	−	−	TTV: 1.3×10^6
30	50	F	after 1 M	24	74	158	0.3	217	0.05	−	−	−	TTV: 6.0×10^3
32	52	M	after 2 W	23	33	479	0.9	330	1.38	±	−	−	HHV-6: 1.3×10^3, HHV-7: 5.2×10^3, TTV: 3.1×10^5
33	44	F	after 1 M	38	44	234	0.9	209	0.10	−	−	−	HHV-6: not detectable, TTV: 1.7×10^5
34	19	M	after 2 M	28	56	160	0.9	146	0.55	−	−	±	TTV: not detectable
35	76	F	after 3 M	29	13	776	1.0	244	0.45	−	−	−	TTV: not reexamined
36	80	M	after 3 W	94	172	258	25.1	272	2.07	±	−	−	HBV: 1.6×10^8, EBV: 1.5×10^3, TTV: 1.76×10^6
37	57	M	after 1 M	16	20	223	0.9	132	0.30	−	−	−	HBV: not reexamined

Normal upper limits of AST: ALT: ALP: T-Bil: LDH: and CRP are 40 IU/L: 40 IU/L: 360 IU/L: 1.3 mg/dL: 230 IU/L: and 0.3 mg/dL: respectively.
AIDS: acquired immunodeficiency syndrome, ALL: acute lymphoblastic leukemia, ALP: alkaline phostphatase, ALT: alkaline transaminase, AML: acute myeloid leukemia, ATL: adult T-cell leukemia, BMT: bone marrow transplantation, CRP: C-reactive protein, FUO: fever of unknown origin, HPS: hemophagocytic syndrome, IP: interstitial pneumonia, LDH: lactate dehydrogenase, LN: lymph node, MDS: myelodysplastic syndrome, PH: pulmonary hypertension, Tbc: tuberculosis, T.Bil: total bilirubin

Intern Med 52: 201-211, 2013 DOI: 10.2169/internalmedicine.52.8206

Table 6. Characteristics of Patients with Normal Liver Function or Mild Dysfunction Regardless of Positive Viral Polymerase Chain Reaction

Patient No.	Age	Sex	Underlying disease	AST	ALT	ALP	T.Bil	LDH	CRP	Fever	Skin rash	LN swelling	Virus detected and its copy number
38	60	M	AML, post BMT	30	78	348	0.7	106	0.17	−	−	−	CMV: 7.6×10^2
39	19	F	AML, post BMT	28	28	205	0.5	383	0.82	−	−	−	HHV-6: 3.1×10^3
40	58	F	Ulcerative colitis	43	40	262	0.2	152	15.95	+	−	−	CMV: 3.5×10^2, EBV: 1.9×10^2
41	44	M	AML, post BMT	45	74	232	1.3	200	0.13	−	±	−	HHV-6: 1.1×10^3, TTV: 1.2×10^2
42	63	F	AML	34	40	260	0.4	204	2.05	±	−	−	HHV-6: 6.5×10^3
43	86	M	MDS/AML	28	46	318	1.1	408	17.52	+	+	−	HHV-6: 4.6×10^3
44	65	M	MPD/AML, post BMT	15	18	218	0.8	149	0.26	−	−	−	TTV: 9.2×10^3
45	58	M	Malignant lymphoma	75	71	328	0.9	174	0.11	−	−	−	HHV-6: 1.1×10^4, TTV: 8.9×10^3
46	58	F	Malignant lymphoma	42	79	164	1.2	187	0.65	±	−	−	TTV: 6.3×10^2
47	74	F	Malignant lymphoma	24	14	157	0.4	2,113	3.97	+	−	−	CMV: 5.9×10^3 TTV: 3.8×10^3, HSV-1: 1.5×10^6
48	67	M	MPD/AML, post BMT	14	19	188	1.3	232	0.14	−	−	−	CMV: 1.0×10^6, HHV-6: 1.9×10^2
49	45	M	AML, post BMT	16	53	190	0.7	188	11.24	+	−	−	TTV: 1.4×10^4

ALP: alkaline phosphatase, ALT: alkaline transaminase, AML: acute myeloid leukemia, BMT: bone marrow transplantation, CRP: C-reactive protein, LDH: lactate dehydrogenase, LN: lymph node, MDS: myelodysplastic syndrome, T.Bil: total bilirubin

HHV-6 load was significantly correlated with the levels of AST, ALT, and ALP between the 1st and 2nd examinations, and the correlation coefficients ranged from 0.9435 to 1.0000. Patient 21 had CMV-infectious mononucleosis, and CMV was undetectable after 2 months of treatment with ganciclovir, with normalized liver function. The liver dysfunction was improved after treatment with ganciclovir in another patient with CMV-infectious mononucleosis (patient 18), although the viral load was not reexamined. Patient 19 had EBV-infectious mononucleosis, and the liver dysfunction was also improved with the resolution of fever and lymph node swelling, suggesting the natural course of this disease. On the other hand, the relationship between the changes in liver dysfunction and the TTV load was unclear in 7 patients in that were re-assayed for TTV, and TTV became undetectable in patient 34 with the improvement of the liver dysfunction.

Incidence of liver dysfunction in each viral infection

Twelve patients that did not exhibit overt liver dysfunction regardless of viremia are described in Table 6. The incidence of TTV, HHV-6, CMV, EBV, and HSV-1 infections were 6/12, 6/12, 4/12, 1/12, and 1/12, respectively. The frequency of individual viral infections was similar to that of the patients with liver dysfunction (Table 4). These results suggested that these viral infections do not always cause overt liver dysfunction; therefore, the incidence of liver dysfunction was calculated in each case of viremia listed in Tables 3, 5. The results showed 70% TTV, 68% HHV-6, 43% CMV, and 83% EBV.

Consistency of the results obtained by multiplex PCR in comparison to those obtained by routine viral examination

The results obtained by multiplex PCR combined with real-time PCR and we compared with those obtained with commercially available virus examinations (Mitsubishi Chemical Medience Corporation, Tokyo, Japan), which are routinely employed in this institute. Attending physicians performed routine virus examinations independent of the current assay system in order to investigate the cause of the liver dysfunction or the inflammation. Table 7 shows that the results obtained with the PCR assay system were consistent with those obtained with routine virus tests except for the results of EBV in patients 18, 21, and 40. EBV was not detectable in the PCR assay in the first 2 patients, while the routine EBV serological test was positive for the VCA-IgM antibody. In contrast, the PCR assay system gave a positive result regardless of the negative VCA-IgM antibody determined by routine examination in patient 40. The assay was re-examined in the first 2 patients with a preserved DNA specimen with negative results. In addition, Table 8 shows that the results for HBV and HCV by the PCR were consistent with those by the commercially available method (SRL Inc., Hachioji, Japan).

In addition, the viral load of ParvoB19 was examined in a patient (52-year-old man) that came to the hospital because of anemia and a very low reticulocyte count. A bone marrow aspirate showed pure red cell aplasia (PRCA) with re-